Optimal Application Conditions for Steam/Solvent Coinjection

Mohsen Keshavarz, Ryosuke Okuno, and **Tayfun Babadagli,** University of Alberta

Summary

Laboratory and field data, although limited in number, have shown that steam/solvent coinjection can lead to a higher oil-production rate, higher ultimate oil recovery, and lower steam/oil ratio, compared with steam-only injection in steam-assisted gravity drainage (SAGD). However, a critical question still remains unanswered: Under what circumstances can the previously mentioned benefits be obtained when steam and solvent are coinjected? To answer this question requires a detailed knowledge of the mechanisms involved in coinjection and an application of this knowledge to numerical simulation. Our earlier studies demonstrated that the determining factors for improved oil-production rates are relative positions with respect to the temperature and solvent fronts, the steam and solvent contents of the chamber at its interface with reservoir bitumen, and solvent-diluting effects on the mobilized bitumen just ahead of the chamber edge. Then, the key mechanisms for improved oil displacement are solvent propagation, solvent accumulation at the chamber edge, and phase transition.

This paper deals with this unanswered question by providing some key guidelines for selecting an optimum solvent and its concentration in coinjection of a single-component solvent with steam. The optimization considers the oil-production rate, ultimate oil recovery, and solvent retention in situ. Multiphase behavior of water/hydrocarbon mixtures in the chamber is explained in detail analytically and numerically. The proposed guidelines are applied to simulation of the Senlac solvent-aided-process pilot and the Long Lake expanding-solvent SAGD pilot.

Results show that an optimum volatility of solvent can be typically observed in terms of the oil-production rate for given operation conditions. This optimum volatility occurs as a result of the balance between two factors affecting the oil mobility along the chamber edge: reduction of the chamber-edge temperature and superior dilution of oil in coinjection of more-volatile solvent with steam. It is possible to maximize oil recovery and minimize solvent retention in situ by controlling the concentration of a given coinjection solvent. Beginning coinjection immediately after achieving interwell communication enables the enhancement of oil recovery early in the process. Subsequently, the solvent concentration should be gradually decreased until it becomes zero for the final period of the coinjection. Simulation case studies show the validity of the oil-recovery mechanisms described. In the final section of the paper, a limited economic analysis of SAGD and different coinjection cases is provided.

Introduction

Steam-assisted gravity drainage (SAGD) is the most-used method for bitumen and heavy-oil recovery in western Canada (Butler 1997). In SAGD, high-quality steam is injected into the reservoir through a horizontal injector and forms a steam chamber. The heated bitumen and condensed water drain along the chamber edge toward a horizontal producer, which is drilled a few meters below the injector. Disadvantages of SAGD include high energy demands and associated environmental costs.

This paper (SPE 165471) was accepted for presentation at the SPE Heavy Oil Conference Canada, Calgary, 11–13 June 2013, and revised for publication. Original manuscript received for review 10 May 2013. Revised manuscript received for review 29 July 2014. Paper peer approved 28 August 2014.

Coinjection of solvent with steam has been studied as a promising alternative to improve the efficiency of SAGD by taking advantage of both heat and solvent-dilution effects on oil viscosity. Coinjection has been studied under various commercial names. Improved oil-production rates and lower steam/oil ratios in coinjection have been reported in the literature (Nasr et al. 2003; Gates 2007; Ivory et al. 2008; Li et al. 2011a, b; Yazdani et al. 2011); they include EnCana's solvent-aided-process (SAP) pilot in Senlac (Gupta et al. 2005; Gupta and Gittins 2006) and in Christina Lake (Gupta and Gittins 2006) and Imperial Oil's liquid-addition-to-steam-enhanced-recovery pilot in Cold Lake (Leaute 2002; Leaute and Carey 2005).

There also exist reports of incremental-oil recovery by coinjection compared with steam-only injection (Redford and McKay 1980; Li and Mamora 2010; Ardali et al. 2012a; Mohammadzadeh et al. 2012; Jha et al. 2013). Keshavarz et al. (2014) explained the detailed mechanisms responsible for the enhanced oil-production rate and local-displacement efficiency in steam/solvent coinjection.

In addition to successful tests of coinjection, there have also been less-successful results found; for example, Nexen's expanding-solvent SAGD (ES-SAGD) test in Long Lake in 2006 was less encouraging than the pilot tests by EnCana and Imperial Oil (Orr 2009; Orr et al. 2010). Suncor's ES-SAGD project in the Firebag area exhibited little improvement in the oil-production rate (Orr 2009).

Coinjection of steam and solvent involves multiphase behavior of solvent/water/bitumen mixtures and their interaction with nonisothermal flow under heterogeneities. Because of its complexity, most of the studies on coinjection design in the literature focus on selection of solvent and its concentration to improve the oil-production rate under simplified reservoir conditions. Nevertheless, there are various different proposals on these two design parameters in the literature, and many of them are specific to the reservoir or to experimental conditions. Different reservoirs, however, should have different optimum sets of operation parameters for successful coinjection. Thus, the main objective of this paper is to propose systematic guidelines to optimize single-component solvent and its concentration in terms of oil-production rate, ultimate oil recovery, and solvent retention (or solvent losses) for given reservoir conditions. To emphasize the diversity of prior proposals and the importance of our research, a brief review of prior studies on coinjection design is provided.

Nasr et al. (2003) considered that the condensation temperatures of solvent and water should be similar to each other at the operational pressure. The idea was to have solvent and steam condense simultaneously near the chamber edge. This criterion has been used in many studies, and C_6 or C_7 were pointed out as the optimum solvent in most of these studies (Li and Mamora 2010; Hosseininejad Mohebati et al. 2010; Li et al. 2011a; Yazdani et al. 2011; Ardali et al. 2012a). A closer investigation of steam/solvent-phase behavior by Dong (2012) showed that the criterion of Nasr et al. (2003) does not result in simultaneous condensation of water and solvent at the chamber edge.

In addition, solvents resulting in the highest drainage rates in other studies are not always consistent with Nasr et al. (2003). Redford and McKay (1980) investigated normal hydrocarbons from methane to pentane and a number of commercial hydrocarbon blends as additives to low-pressure steam. They reported that coinjection of heavier hydrocarbon blends resulted in improved bitumen production from Athabasca oil sand, provided enough light blends were also present. They properly made mention of

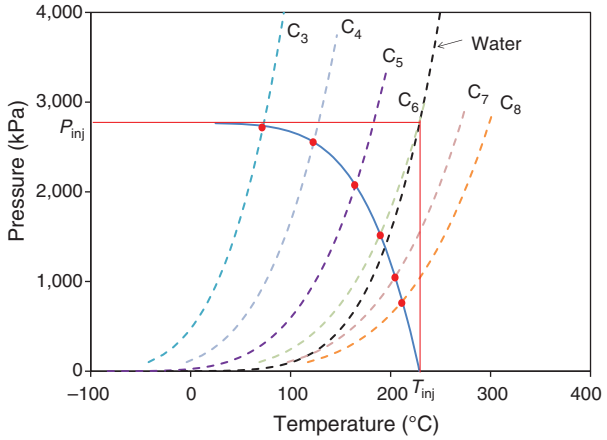

Fig. 1—Example for solutions of Eq. 2 for a few different single-component solvents at an injection pressure P_{inj}. Dashed curves are vapor pressures of water and a few solvent components. The bold solid curve shows $P_{inj} - P^{vap}_{water}$, where P^{vap}_{water} is the vapor pressure of water. The dot on the vapor-pressure curve of each solvent represents the solution of Eq. 2 for *L*/*V*/*W* equilibrium (T_{3p}) when that solvent is coinjected with steam. T_{3p} corresponds to the chamber-edge temperature. T_{inj} = injection temperature.

the dependency of solvent selection on pressure/volume/temperature properties of the fluid system. Promising results from addition of heavy solvents to steam were also reported by Li et al. (2011b). Results of Shu and Hartman (1988) showed that medium solvents (such as naphtha) gave the best results in the total oil production at a somewhat greater solvent loss. They observed little improvement in oil recovery with heavy solvents (i.e., $C_{16–20}$).

Some studies indicated a superior performance of lighter solvents. For example, Govind et al. (2008) reported an additional improvement in the oil-production rate when C_4 is coinjected with steam over that obtained from coinjection of C_5 and heavier hydrocarbons at the operating pressure of 4000 kPa. Ardali et al. (2010) studied coinjection of *n*-alkenes from C_3 to C_7 with steam and concluded that C_4 was suitable for coinjection at Cold Lake at the operating pressure of 3400 kPa, and heavier solvents were suitable for Athabasca reservoirs at the operating pressure of 2100 kPa.

Many proposals also exist for coinjection procedures with different concentrations of coinjected solvents (Gates and Chakrabarty 2008; Gates and Gutek 2008; Gupta and Gittins 2007a, b; Edmunds et al. 2010; Jiang et al. 2012). Some of the research considered how to minimize solvent retention in the reservoir (or solvent loss).

The diversity of these prior proposals indicates the need for a systematic procedure for designing solvent and its injection procedure. The next section describes the condensation behavior of steam and solvent in coinjection with a SAGD-type well pattern, which can significantly affect the oil-production rate. Then, selection of solvent is made mainly to optimize the oil-production rate. An injection procedure for the selected solvent is also presented to maximize ultimate oil recovery while minimizing both dynamic and ultimate solvent retention in situ. Finally, case studies show applications of the systematic procedure to two actual field cases: EnCana's SAP pilot in Senlac (Gupta et al. 2005; Gupta and Gittins 2006) and Nexen's ES-SAGD pilot in Long Lake (Nexen 2007; Orr et al. 2010). The last section of the paper presents a limited economic analysis of SAGD and different coinjection cases.

Condensation Behavior of Steam and Solvent in Coinjection

Coinjection can exhibit a chamber-edge temperature that is substantially lower than that in steam-assisted gravity drainage (SAGD) (Keshavarz et al. 2014). Dong (2012) explained an altered temperature distribution in coinjection by use of simplified representation of binary phase behavior of water and a single-component solvent. Because the oil drainage occurs along the chamber edge, reliable estimation of fluid properties at the chamber edge is important in selecting an appropriate solvent to be coinjected with steam.

This section presents an application of the analysis of Dong (2012) for estimation of the chamber-edge temperature for a wide variety of solvents and operating conditions. The estimations are then compared with results from numerical flow simulations, where some of the assumptions made in the estimation are relaxed.

Assumptions are made as follows: binary mixtures of water and a single-component solvent; Raoult's law for phase equilibrium; no mutual solubility between water and solvent; and a negligible pressure gradient in the chamber. The phase-equilibrium relation for component *i* can then be written as

$$P_i^{vap} = y_i P, \quad \ldots\ldots\ldots\ldots\ldots\ldots\ldots\ldots\ldots\ldots\ldots\ldots (1)$$

where P_i^{vap} is the vapor pressure of component *i*, P is the system pressure, y_i is the mole fraction of component i in the gaseous phase, and i is the component index (i.e., i = water, solvent). Eq. 1 is for the aqueous (W) and gaseous (V) phases for i of water, and also for the oleic (L) and gaseous (V) phases for i of solvent. By definition, $\sum_i y_i = 1.0$, or $\sum_i y_i P = P$. By use of Eq. 1, we have

$$P = \sum_i P_i^{vap}. \quad \ldots\ldots\ldots\ldots\ldots\ldots\ldots\ldots\ldots\ldots\ldots\ldots (2)$$

Vapor-pressure curves for the water and solvent compounds can be expressed as functions of temperature by use of an equation of state or by correlations, such as Antoine's correlation (Linstorm and Mallard 2011). Eq. 2 can then be solved for the temperature for the *L*/*V*/*W* equilibrium (T_{3p}) at a given pressure. Once T_{3p} is obtained, Eq. 1 gives the component mole fractions in the V phase at that pressure and T_{3p}. An example calculation is given in Appendix A with C_4 as the solvent component.

T_{3p} corresponds to the chamber-edge temperature for coinjection of steam and a certain solvent compound under consideration. Ahead of the chamber edge, temperature is lower than T_{3p}, and there exist two immiscible liquid phases (i.e., the L and W phases). Inside the chamber, temperature is higher than T_{3p}, and the two equilibrium phases consist of either V and L or V and W, depending on the overall composition. Details of relevant phase diagrams can be found in Dong (2012). Note that bitumen is not considered in the system here because of our first assumption: binary mixtures of water and a single-component solvent. As stated by Dong (2012), the temperature and partial pressure of steam or solvent at the chamber edge are independent of the initial concentration of solvent in the injectant under the assumptions made.

Fig. 1 shows the solutions of Eq. 2 at an injection pressure P_{inj} for binaries of water and a few different hydrocarbons. T_{3p} at P_{inj} is where $(P_{inj} - P^{vap}_{water})$ intersects $P^{vap}_{solvent}$. **Fig. 2** summarizes the T_{3p} solutions for different solvents at different injection pressures. These plots should be interpreted only for temperatures higher than the initial reservoir temperature. Coinjection of a more-volatile solvent results in a lower temperature at the chamber edge. Coinjection of a given solvent at a lower pressure gives a smaller reduction in the chamber-edge temperature.

Fig. 3 shows the water-component mole fractions in the V phase at the chamber edge for different solvents at different injection pressures. Gradual condensation of water in the chamber causes the V phase to become richer in the solvent component. Coinjection of a more-volatile solvent results in a lower concentration of water in the V phase near the chamber edge. This is because a more-volatile solvent has a higher K-value at a fixed P and the corresponding T_{3p} (i.e., $K_{solvent} = P^{vap}_{solvent}/P = y_{solvent} = 1.0 – y_{water}$) under the assumptions made. This concentration profile is not very sensitive to the injection pressure in Fig. 3. This is also a direct result of the condensation behavior of the water and solvent components, which is described by the vapor-pressure curves in this simple phase-behavior model.

Some prior studies explained that reduction of the chamber-edge temperature in coinjection occurs because of a reduced partial pressure of water in the V phase (i.e., $y_{water} < 1.0$). However,

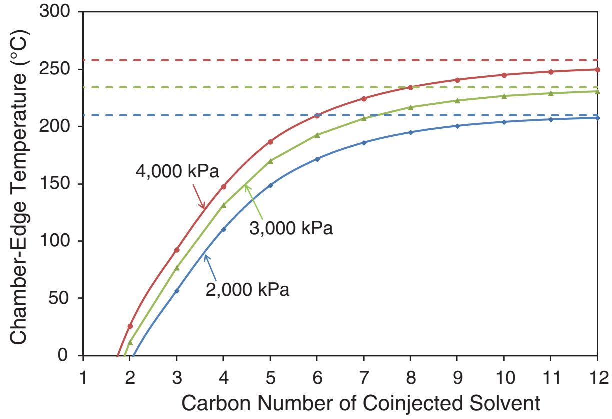

Fig. 2—Chamber-edge temperatures estimated by use of Eq. 2 for single-component solvents from C_1 through C_{12} for injection pressures of 2.0, 3.0, and 4.0 MPa. The horizontal asymptote of each curve is shown by a dashed line, which is the chamber-edge temperature for steam-only injection at that pressure. The vertical distance between each data point and its respective horizontal asymptote is the temperature reduction at the chamber edge with respect to steam-saturation temperature at P_{inj}. This reduction is more severe as the solvent becomes more volatile for a given injection pressure and as the injection pressure increases for a given single-component solvent. The plots are used for temperatures greater than the original reservoir temperature.

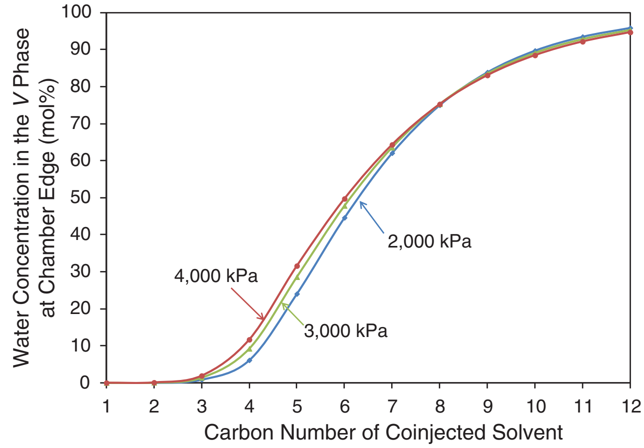

Fig. 3—Water mole fraction in the *V* phase at the chamber edge for coinjection of a single-component solvent and steam. Dots are solutions of Eq. 1 after solving Eq. 2 for T_{3p}. Coinjection of a more-volatile solvent results in a lower concentration of water in the *V* phase near the chamber edge.

the most fundamental reason is the deviation of T_{3p} from the steam temperature at a given injection pressure, as shown in the sequential solution of Eqs. 1 and 2 and in Fig. 1.

Some of the assumptions made earlier are invalid for many practical applications. The STARS simulator (CMG 2011) is used to see how the assumptions, especially our first two assumptions, can affect the accuracy of the chamber-edge-temperature estimation based on Dong (2012).

A 2D homogeneous reservoir of 70.0×37.5×20.0 m with gravity is considered, with a uniform gridblock size of 1.0×37.5×1.0 m. The injector and producer are at the left boundary at depths of 16 and 20 m from the top, respectively (i.e., only one-half of a steam chamber is simulated in this section). Reservoir/fluid properties used are presented in **Table 1.** Capillarity and physical diffusion/dispersion are not considered in this research.

A typical viscosity-vs.-temperature relation for Athabasca bitumen is estimated by use of Eq. 3 (Mehrotra and Svrcek 1986):

$$\ln\mu = \exp(A + B\ln T), \quad (3)$$

where μ is bitumen viscosity in cp and T is the absolute temperature in Kelvin. The constants used, A and B, are 22.8515 and −3.5784, respectively. The bitumen considered here is a dead oil (i.e., only solvent and water can exist in the *V* phase). Fluid-phase behavior is represented by use of constant-*K* flash with the Rachford and Rice equations (Rachford and Rice 1952). Tabulated *K*-

Properties	Values
Porosity	33%
Horizontal permeability	4,000 md
Vertical permeability	3,000 md
Initial reservoir pressure at depth of 500 m	1500 kPa
Initial reservoir temperature	13°C
Initial oil saturation	0.75
Initial water saturation	0.25
Residual oil saturation	0.13
Three-phase relative permeability model (CMG 2011)	Stone's Model II
Formation compressibility	1.8E–5 1/kPa
Rock heat capacity (Butler 1997)	2600 kJ/m^3 °C
Rock thermal conductivity (Butler 1997)	660 kJ/m-d °C
Over-underburden heat capacity (Butler 1997)	2600 kJ/m^3 °C
Over-underburden thermal conductivity (Butler 1997)	660 kJ/m-d °C
Bitumen thermal conductivity (Butler 1997)	11.5 kJ/m-d °C
Gas thermal conductivity (Yazdani et al. 2011)	2.89 kJ/m-d °C
Water thermal conductivity	1500 kJ/m-d °C
Bitumen molecular weight (Mehrotra and Svrcek 1987)	594.6 kg/kg-mole
Bitumen specific gravity (Mehrotra and Svrcek 1987)	1.077
Injector bottomhole pressure (maximum)	2730 kPa
Producer bottomhole pressure (minimum)	1500 kPa
Producer steam-flow rate (maximum)	1 m^3 (CWE)/d
Steam quality	0.9

Table 1—Reservoir and fluid properties used in numerical simulations.

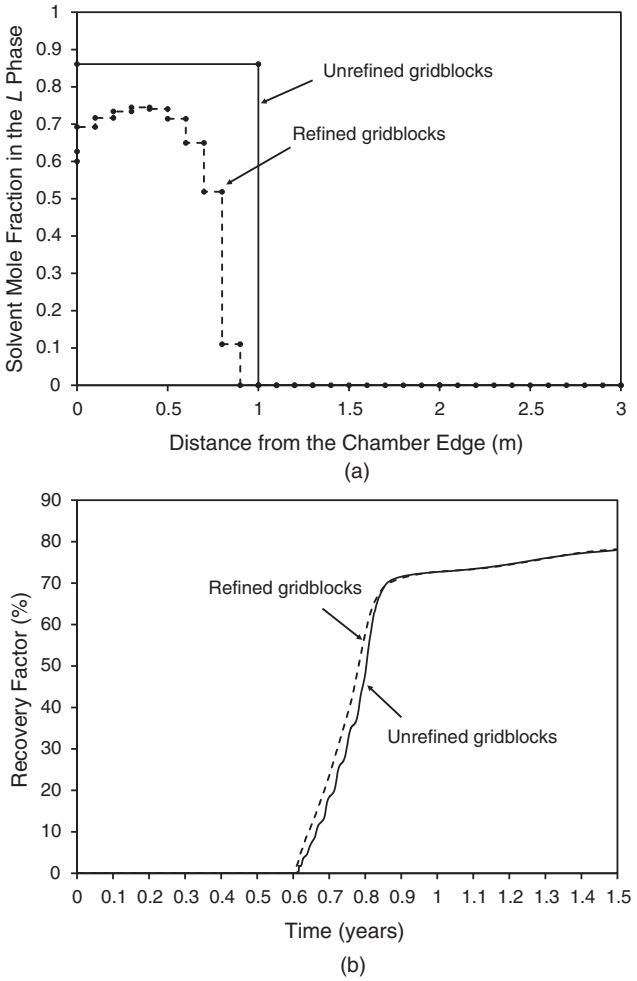

Fig. 4—Effect of grid refinement on the results of C_5/steam-coinjection simulation. (a) Solvent distribution in the *L* phase beyond the chamber edge after 10 months; (b) bitumen-recovery factor. Gridblock length in the *i*-direction is reduced from 1 m in the original case to 0.1 m in the refined case. Also, the length of the reservoir model is reduced to 10 m for both cases to reduce the simulation time. (a) The length scale of the solvent/bitumen-mixing zone is approximately 1 m, which is considerably greater than that predicted by considering molecular diffusion alone. This region becomes even thicker as the chamber grows with further solvent accumulation. (b) The effect of grid refinement is insignificant on oil recovery in this case.

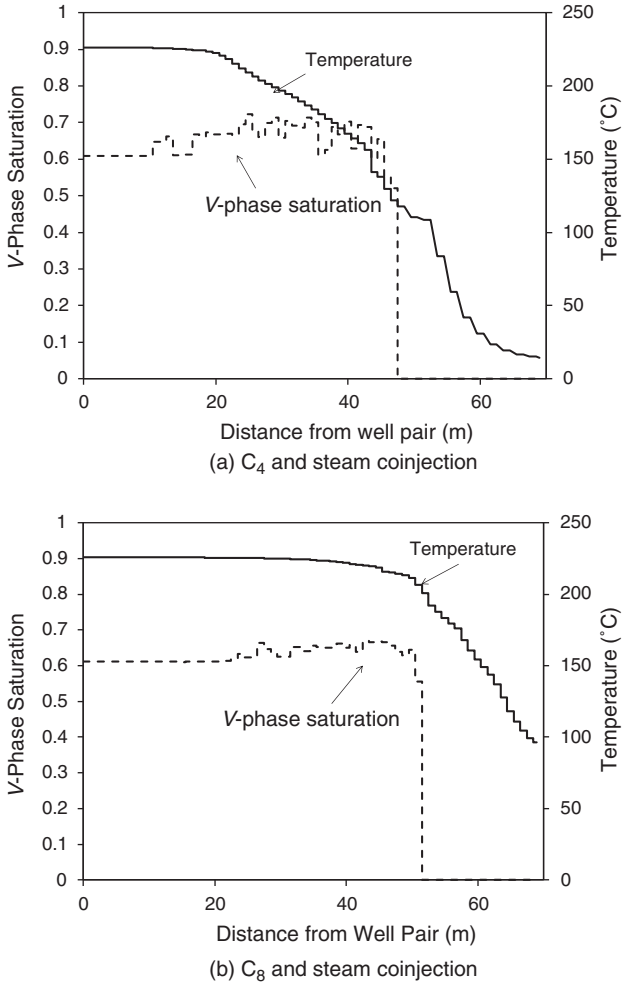

Fig. 5—Variations of temperature and the *V*-phase saturation simulated along the sixth row from the top of the reservoir model at 2 years. The C_4- and C_8-coinjection cases are shown in (a) and (b), respectively. The chamber edge is defined where the *V*-phase saturation becomes zero on the phase transition between three and two phases. The temperature in the gridblock just before the gridblocks without the *V* phase is considered to be the chamber-edge temperature. The chamber-edge temperature is 122°C in (a), where C_4 is coinjected with steam at 2730 kPa, and it is 207°C in (b), where C_8 is coinjected with steam at 2730 kPa.

values are generated by performing a series of flash calculations by use of the Peng-Robinson equation of state (Peng and Robinson 1976) with the van der Waals mixing rules for hydrocarbons. Raoult's law is used for *K*-values for the water component. Possibilities of mutual solubility of water and hydrocarbons and asphaltene precipitation are not considered in this study.

Well constraints are given in Table 1. The injected steam has a quality of 0.9 and temperature of 228.7°C. Preheating of the reservoir is performed for 6 months. Simulations are performed for steam-only injection and steam/solvent coinjection with different single-component solvents from C_3 to C_8 for 5 years. The solvent concentration in the injection stream is 2 mol% in all cases unless otherwise stated.

The solvent condensed at the chamber edge is mixed with reservoir-oil components in the *L* phase. The reservoir mixing is caused by molecular diffusion and is enhanced by spreading mechanisms with convection, as discussed by Garmeh and Johns (2010) and Adepoju et al. (2013). In steam/solvent coinjection, this convection is mainly the gravity drainage along the chamber edge. The transverse dispersion associated with the gravity drainage is likely the main driving force for spatial distribution of condensed solvent beyond the chamber edge. This transverse dispersion could make the length scale of the solvent/bitumen mixing zone several orders of magnitude greater than that of the molecular diffusion. Gupta and Gittins (2012) have also reported that a larger mixing zone of solvent and bitumen should be considered around the chamber interface to explain the results obtained from field application and numerical simulations of coinjection. To see the effect of the number of *i*-direction gridblocks on C_5-coinjection simulation, **Fig. 4** gives C_5 concentrations beyond the chamber edge and oil recoveries for the two cases: one with the *i*-direction gridblock length of 1.0 m (the base case) and the other with 0.1 m. Considering the small differences in simulation results, it is concluded that the original reservoir gridding (the base case) is appropriate for the current simulation studies. Proper modeling of component mixing near the chamber edge is an important technical issue to be resolved. However, this is beyond the scope of this paper.

Fig. 5 presents variations of temperature and the *V*-phase saturation simulated along the sixth row from the top of the reservoir model at 2 years for the C_4- and C_8-coinjection cases, respectively. The chamber edge is defined where the *V*-phase saturation becomes zero on the phase transition between three and two

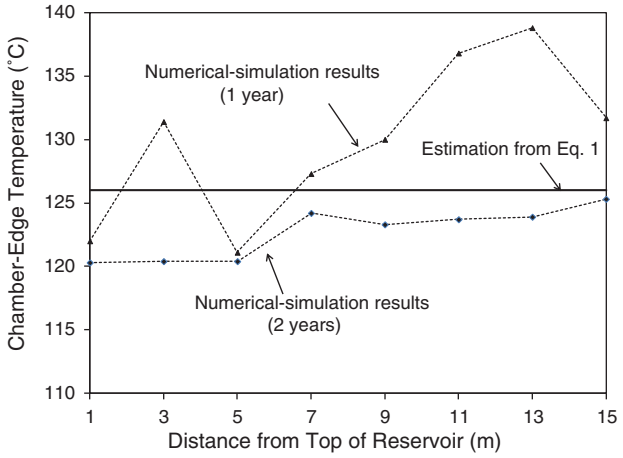

Fig. 6—Comparison of numerical-simulation results and estimations from Eq. 2 for the chamber-edge temperature. C_4 is the coinjected solvent. Results are presented for different rows of the reservoir model at 1 and 2 years. The assumptions made for Eq. 2 result in an error range of ±15°C in the cases studied.

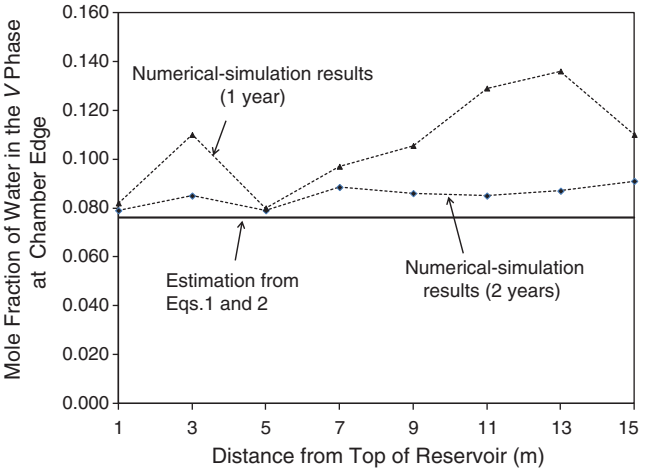

Fig. 7—Comparison of numerical-simulation results and estimations from Eq. 1 for the water mole fraction in the *V* phase at the chamber edge. C_4 is the coinjected solvent. Results are presented for different rows of the reservoir model at 1 and 2 years.

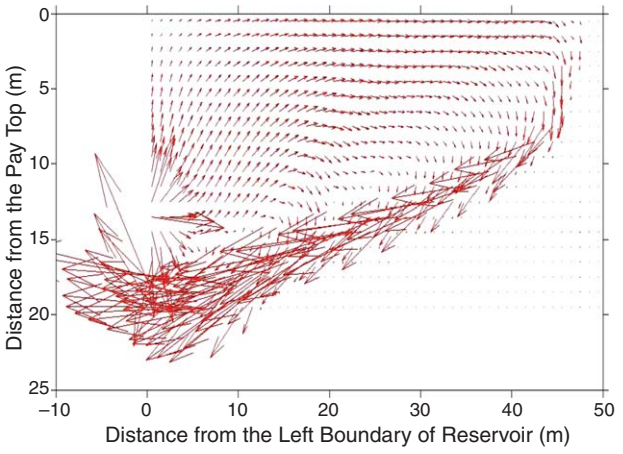

(a) c_4 and steam coinjection, 23 months from the start of simulation

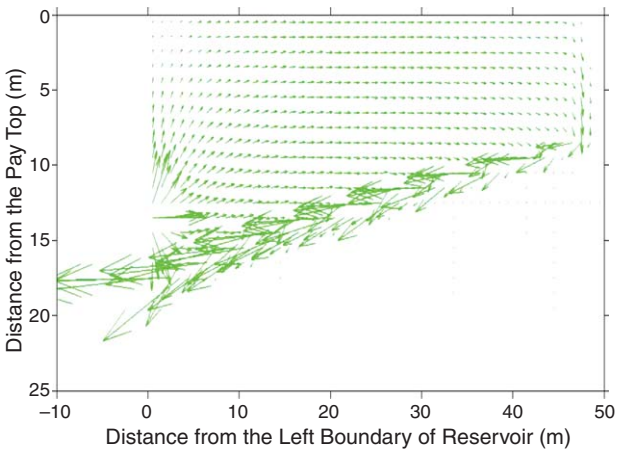

(b) steam-only injection, 23 months from the start of simulation

Fig. 8—Water molar fluxes in steam-only injection and the C_4/steam-coinjection cases. The well pair is at the left boundary of the reservoir. Horizontal axis shows the distance from the left boundary, and the vertical axis shows the distance from the top of the reservoir model. Arrows represent the direction and the magnitude of water molar fluxes. Lengths of arrows cannot be compared among different cases because they have different scales. Downward deviation of fluxes indicates a greater fraction of water-component flux comes from the *W* phase. This effect becomes more pronounced as the coinjected solvent becomes more volatile.

phases. The chamber-edge temperature is 85°C lower for the C_4-coinjection case than for the C_8-coinjection case. Fig. 5a also indicates that condensation of water starts deep inside the chamber.

Fig. 6 compares the chamber-edge temperatures estimated from Eq. 2 and those from simulation for coinjection of C_4 and steam. The estimation from Eq. 2 gives an error range of ±15°C, compared with the simulation results. **Fig. 7** presents a similar comparison for the water mole fractions in the *V* phase at the chamber edge. The accuracy of the component mole fractions calculated from Eq. 1 is affected by an error in estimation of the chamber-edge temperature. Fig. 7 shows that Eq. 1 systematically underestimates the water mole fractions in the *V* phase at the chamber edge for the case studied. The deviations observed in Figs. 6 and 7 indicate that the mutual solubility between the dead oil and solvent and fluids' nonidealities can affect physical properties at the chamber edge and oil-recovery predictions in coinjection.

Fig. 8 presents the water molar fluxes in steam-only injection and the C_4/steam coinjection. Arrows represent the direction and the magnitude of water molar fluxes. Note that lengths of arrows cannot be compared among different cases because they have different scales. The effect of gravity on the water flux comes mainly from the condensed *W* phase; thus, downward fluxes in the C_4 coinjection in Fig. 8a indicate that a greater fraction of the water-component flux comes from the *W* phase compared with SAGD. This effect is more pronounced for lighter solvents, for which less energy is transported to the chamber edge by steam.

Our first assumption, binary mixtures of water and a single-component solvent, leads to a simplification that only water and the single-component solvent can exist in the *V* phase. This will be invalid when multicomponent solvent is considered and when some components in the reservoir oil can be present in the *V* phase at high concentrations.

Solvent Selection

Coinjection attempts to enhance the oil-production rate through two main measures: heat and dilution of oil with solvent. As discussed previously, coinjection of a more-volatile solvent tends to result in a lower temperature and steam availability in the vicinity of the chamber edge for given operating conditions. A less-volatile solvent, however, results in a more-viscous mixture when mixed with bitumen at a given mixing ratio at a temperature and pressure. Thus, an optimum volatility of solvent is expected to exist in terms of the oil-production rate for given operating conditions.

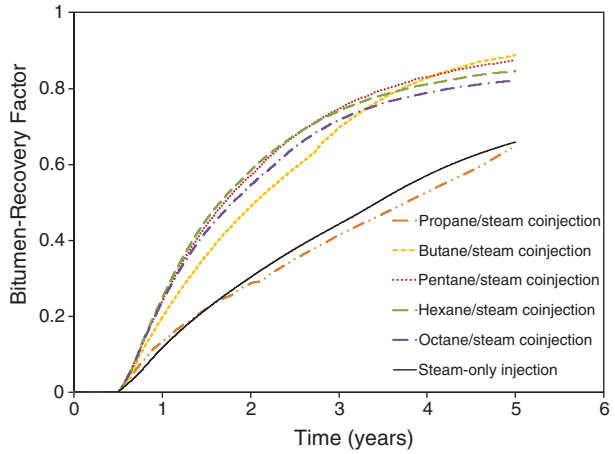

Fig. 9—Oil recoveries for the steam-only injection and coinjection cases with a well-pair spacing of 140 m. Solvent production is excluded in the oil-recovery calculation. Reservoir and fluid properties used are given in Table 1. The solvent concentration in the coinjection stream is 2.0 mol%. The higher ultimate recovery in the C_4/steam coinjection results from the better oil-displacement efficiency (i.e., a lower average S_o) by the end of the project. However, the C_4/steam coinjection exhibits slower chamber propagation than the C_5-, C_6-, and C_8-coinjection cases in the early stage.

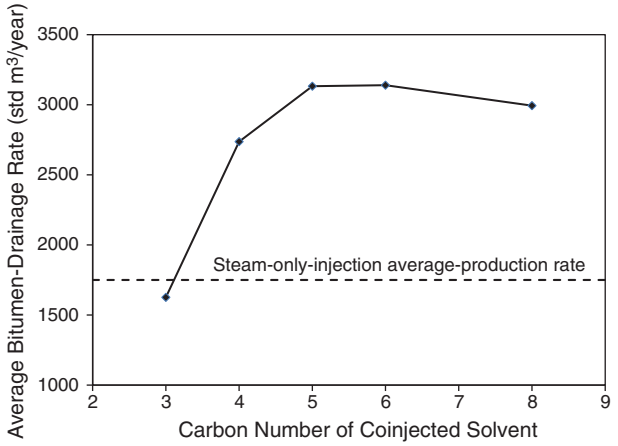

Fig. 10—Average bitumen-production rates for the first 2.5 years in Fig. 8. Results correspond to one-half of the chamber only. The bitumen-production rate is affected by coupled effects of heat and solvent dilution on the mobility of the draining *L* phase near the chamber edge. The breakover point in this figure occurs when these two effects find a balance. The average production rate for steam-only injection is shown with a horizontal line.

In this section, simple simulations of coinjection are performed with different single-component solvents to determine whether such an optimum solvent volatility can be observed. Reservoir properties used are the same as in the preceding section. The following mixing rule is used in the simulations to estimate the viscosity of phase j (μ_j):

$$\ln\mu_j = \sum_{i=1}^{N_C} x_{ij}\ln\mu_{ij}, \quad \ldots\ldots\ldots\ldots\ldots\ldots\ldots\ldots\ldots\ldots (4)$$

where N_C is the number of components, x_{ij} is the mole fraction of component i in phase j, and μ_{ij} is the viscosity of component i in phase j.

Fig. 9 shows oil recoveries simulated with different solvents. The amount of produced solvent is excluded in the calculation of the oil-production rate. **Fig. 10** shows the average oil-production rates from one-half of the chamber in these cases. The average production rate is calculated for the first 2.5 years, when reservoir-boundary effects on chamber propagation are insignificant. Most of the coinjection cases result in higher average production rates for the first 2.5 years than steam-only injection, but coinjection of C_3 yields no improvement in the average production rate.

The cutoff time in Fig. 10 is approximately 20 months after the steam-assisted-gravity-drainage (SAGD) chamber reaches the boundary of the reservoir. For greater well-pair spacing, the averaging may be performed over a longer period of time. **Fig. 11** presents the average bitumen-drainage rates during the first 6 years of the project when a well-pair spacing of 280 m is used. The average production rates in all cases are lower than those in Fig. 10. This is mainly because a larger width/height ratio of the chamber used to generate Fig. 11 makes the resulting average drainage rate lower. Also, there is an improvement observed in the relative performance of C_3/steam coinjection with respect to SAGD. Its cumulative oil production overtakes that of SAGD in the second half of the project time. This is mainly because a larger fraction of the chamber exhibits the enhanced displacement efficiency when larger well-pair spacing is used.

The average bitumen-production rate increases as the coinjected solvent becomes less volatile up to C_6. This is because of the combined effects of temperature, the solubility of solvent in oil, and the solvent-diluting capability on the mobilization of the draining L phase. The solubility of solvent in the L phase at the chamber edge was not discussed in the preceding section because the presence of bitumen was neglected. A discussion is presented here to interpret the simulation results.

At a fixed pressure and temperature, a higher solubility in the L phase is expected for a heavier solvent. However, the average chamber-edge temperature becomes higher as the solvent becomes heavier. This is beneficial for viscosity reduction and transverse mixing of solvent and bitumen, but it adversely affects the solubility of the solvent in the L phase. When the less-effective dilution characteristics of the heavier solvents are also taken into account, the use of heavier solvents can negatively affect the production rate.

To further clarify this point, the C_6/steam-coinjection and C_8/steam-coinjection cases are considered. They result in the average chamber-edge temperatures of 180 and 200°C, respectively, according to the numerical-simulation results. This temperature difference causes only a few centipoises of difference in the bitumen viscosity; however, it causes the average concentration of C_8 in the L phase to be lower than that of C_6 (C_6 and C_8 mole fractions in the L phase are approximately 0.94 and 0.89, respectively, at their corresponding chamber-edge temperature and pressure). In addition, the viscosity of C_8 is greater than that of C_6 at their respective chamber-edge temperatures. Considering significant

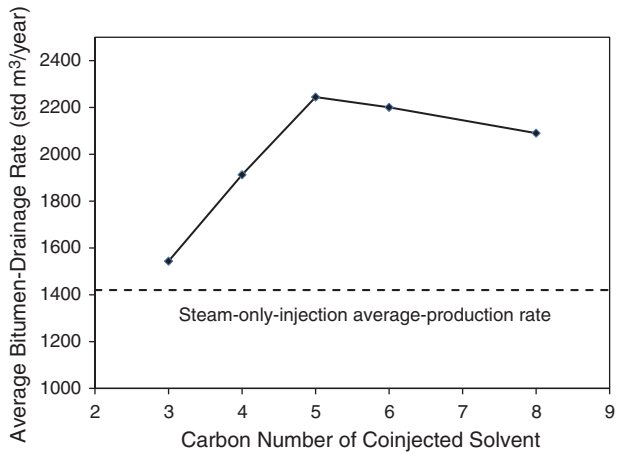

Fig. 11—Average bitumen-production rates for the first 6 years of the projects when a well-pair spacing of 280 m is used. Results represent one-half of the chamber. All simulation cases show a reduction in oil-production rate compared with Fig. 10.

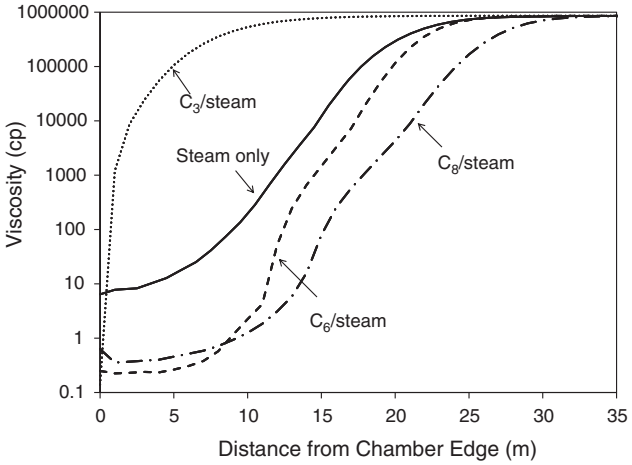

Fig. 12—Profiles of the *L*-phase viscosities in the 12th row of the reservoir model at 1.5 years. The main portion of oil drainage occurs within a few meters of the chamber edge. Thus, the *L*-phase viscosity in this region has a significant effect on the drainage rate. Solvent-dilution effects cannot offset the negative effects of a lowered temperature at the chamber edge for the C_3-coinjection case. The *L*-phase viscosity right ahead of the chamber edge is higher in C_3/steam coinjection compared with that in steam-only injection.

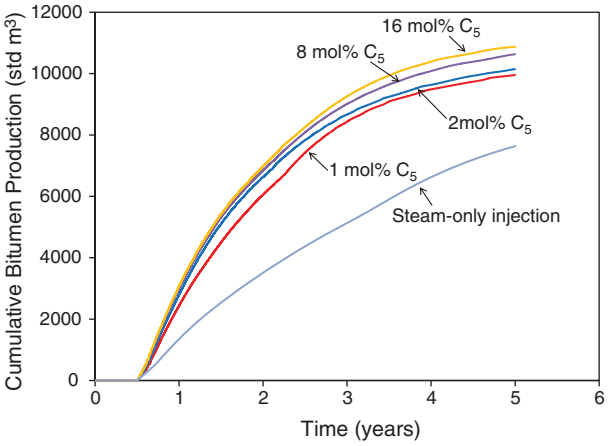

Fig. 13—Comparison of cumulative oil production for steam-only injection and C_5/steam coinjection with different molar concentrations. Results correspond to one-half of the chamber. Increasing the concentration of solvent in the injectant improves oil-production rate.

accumulation of solvent in the *L* phase in this region, a higher viscosity of this phase can occur for coinjection of C_8, compared with that of C_6 **(Fig. 12).** This results in the breakover point in Fig. 10.

The low oil-production rate in the C_3-coinjection case is mainly because the temperature near the chamber edge is much lower than that in the steam-only injection case. The chamber-edge temperature estimated from the preceding section is 72°C for the C_3-coinjection case. The reservoir oil and C_3 have viscosities of approximately 1,060 cp and 0.09 cp at this temperature, respectively. In the steam-only injection case, however, the chamber-edge temperature is 228°C, at which the oil viscosity is only 6 cp. The mixing of solvent and bitumen beyond the chamber edge can depend significantly on the viscosity of bitumen. The mixing zone beyond the chamber edge will be thinner on average for cases with lower chamber-edge temperatures. Thus, depending on temperature and solvent distributions ahead of the chamber, it is highly conceivable that the *L* phase in the C_3-coinjection case becomes more viscous than that in steam-only injection (Fig. 12). This effect will be more severe if lighter solvents (such as C_2 and C_1) are coinjected with steam, as reported in literature (Jiang et al. 1998; Canbolat and Akin 2002; Hosseininejad Mohebati et al. 2010; Li et al. 2011a). Coinjection of noncondensable gases with steam into a bitumen reservoir can lead to slow chamber propagation.

Fig. 10 indicates a simple way to find an optimum volatility range of coinjection solvent in terms of the bitumen-production rate. An optimum solvent in this type of figure will occur when the effects of heating and solvent dilution on oil viscosity find a balance. Although it is not our objective to single out a specific solvent as an optimum, Fig. 10 indicates that solvents lighter than C_4 and heavier than C_6 are not recommended in terms of oil-production rates for the simple simulation case studied here.

Reliable selection of an optimum solvent in terms of the bitumen-production rate also requires accurate prediction of viscosities for bitumen/solvent mixtures at different temperatures, which in itself is a technical issue to be addressed. Also, diffusion and dispersion in the *L* phase can affect the viscosity profile of the *L* phase near the chamber edge. The bitumen studied here is a dead oil with no initial gas/oil ratio. Nonzero initial gas/oil ratio will also shift the breakover point in Fig. 10 because of a lower bitumen viscosity at the initial conditions and altered equilibrium conditions at the chamber edge, both of which affect the drainage rate of the *L* phase. The reservoir thickness is another factor that may affect the efficiency of the process. The cumulative steam/oil ratio of the C_5-coinjection case increases from approximately 2.5 to more than 3.0 when the reservoir thickness is reduced from 20 to 15 m. Sensitivity of the oil-production rate to these additional factors should be considered. Nevertheless, the simple procedure presented here and in Fig. 10 captures the primary effects on the oil mobility in coinjection, and can be extended to other cases considering additional engineering factors.

Design of Solvent Concentration

Coinjection of steam and solvent can achieve oil saturations lower than the residual saturation in the chamber (Redford and McKay 1980; Nasr and Ayodele 2006; Li and Mamora 2010; Ardali et al. 2012a; Mohammadzadeh et al. 2012; Jha et al. 2013). Keshavarz et al. (2014) showed that the oil-saturation reduction results mainly from two processes: solvent accumulation in the *L* phase at the chamber edge and phase transition at the chamber edge between the *W*/*L* equilibrium and the *W*/*L*/*V* equilibrium. The solvent accumulation lowers the oil-component concentrations. The diluted oil is then redistributed in the *V* and *L* phases in the presence of the *W* phase on the phase transition. The equilibrium *L* phase contains a fair amount of oil components; however, the amount of the *L* phase can be significantly small, resulting in low oil saturations in the coinjection chamber.

Accumulation of coinjected solvent occurs because of a higher solvent-injection rate than its drainage rate. This section shows that it is possible to maximize oil recovery and minimize solvent retention in situ by controlling the concentration of a given coinjection solvent. The simulation case discussed in the previous sections, with C_5 as a coinjection solvent, is used in this section.

Fig. 13 compares oil-recovery predictions for different concentrations of C_5 in the injectant. The concentration is constant with time for each simulation case. As the solvent concentration increases, the oil-production rate and oil recovery are both further improved, compared with the steam-only injection case. The use of a higher solvent concentration expedites the accumulation of solvent outside the chamber edge, and oil recovery can be enhanced earlier in the process. Thus, a greater portion of the swept area, including regions closer to the well pair, can exhibit lowered oil saturation compared with the steam-only injection case. A secondary effect of a thicker solvent-rich bank ahead of the chamber edge is a slight improvement in the bitumen-drainage rate.

Fig. 14 shows distributions of the solvent-rich bank at the chamber edge, the *L*-phase saturation inside the chamber, and the temperature for 1 mol% and 8 mol% C_5 coinjections. Fig. 14 confirms that a higher concentration of solvent in the injectant promotes solvent accumulation in the *L* phase just ahead of the

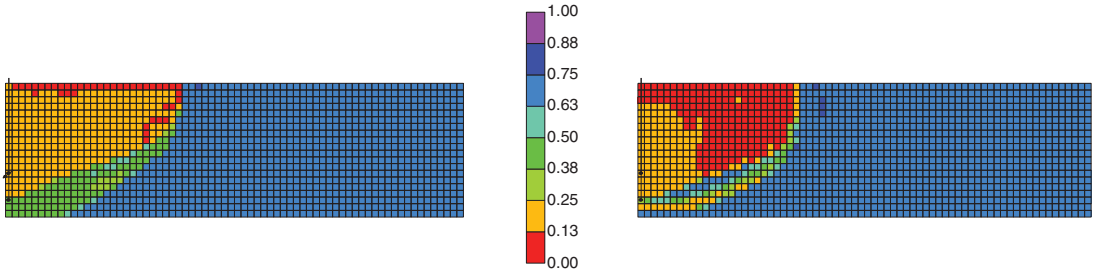

(a) Distributions of the *L* phase saturation in C_5-steam coinjection at 1 year; Left: C_5 concentration of 1 mol%, Right: C_5 concentration of 8 mol%. Regions in red indicate enhanced local displacement efficiency with the *L* phase saturations below S_{or}. The higher C_5 concentration gives higher local displacement efficiency.

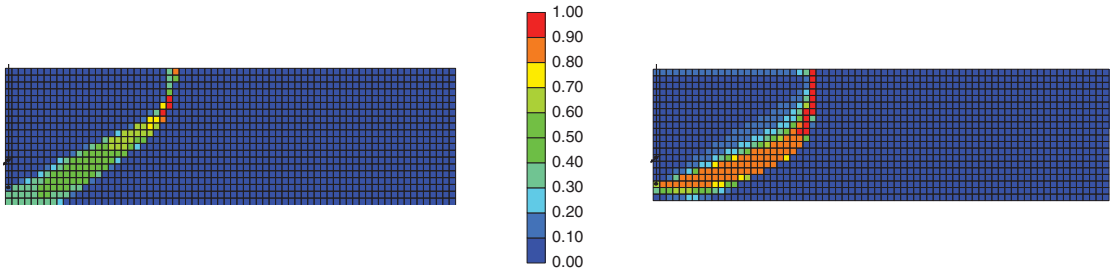

(b) Distributions of the C_5 mole fraction in the *L* phase for C_5-steam coinjection at 1 year; Left: C_5 concentration of 1 mol%, Right: C_5 concentration of 8 mol%. The higher C_5 concentration gives a thicker region of solvent accumulation near the chamber edge.

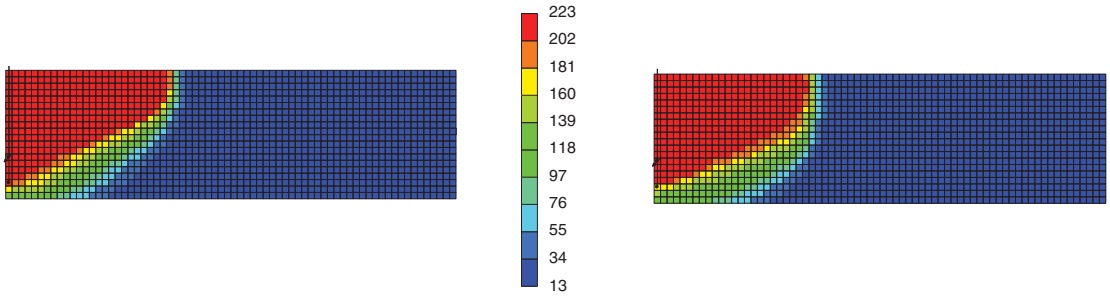

(c) Distributions of temperature at 1 year; Left: C_5 concentration of 1 mol%, Right: C_5 concentration of 8 mol%.

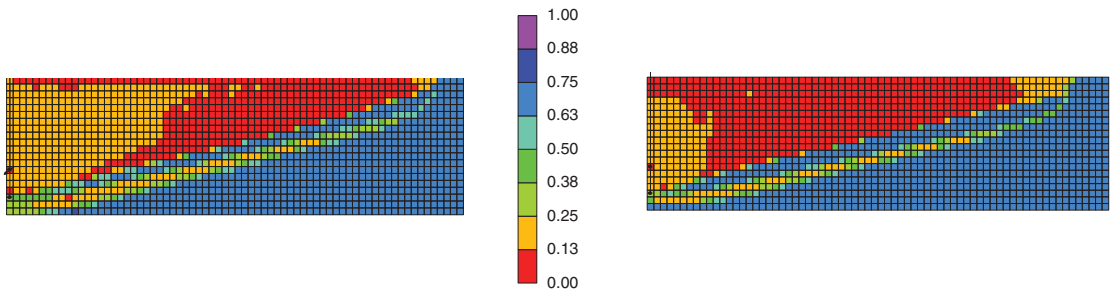

(d) Distributions of the *L* phase saturation in C_5-steam coinjection at 2 years; Left: C_5 concentration of 1 mol%, Right: C_5 concentration of 8 mol%. Regions in red indicate enhanced local displacement efficiency with the *L* phase saturations below S_{or}. Local displacement efficiency is improved in the near-well region for the higher concentration case. The reason for the displacement efficiency not being improved in the small region at the top corner edge of chamber is that temperature has not risen up sufficiently because of accumulation of solvent in this region.

Fig. 14—Distributions of the *L*-phase saturation, solvent (C_5) mole fraction in the *L* phase, and temperature in solvent/steam-coinjection simulations at 1 and 2 years.

chamber edge. This results in improved local-displacement efficiency in the region closer to the well pair and a thicker solvent-rich bank during the process.

In practice, it would not be feasible to coinject a solvent at a high concentration throughout the project period. Results of numerical simulations indicate that use of a higher solvent concentration in the injectant results in a larger amount of solvent retention for a given oil recovery. Solvent retention at a given time is defined as the standard volume of solvent injected minus the standard volume of solvent produced. A solvent concentration of 16 mol% resulted in a cumulative volume of solvent injection approximately four times the cumulative oil production by the end of the process. The injected solvent can be partially recovered as the hot emulsion and gas produced. The recovered solvent may be used for reinjection or to enhance the flow of the sale oil at lower temperatures in pipelines. Simulations showed that the

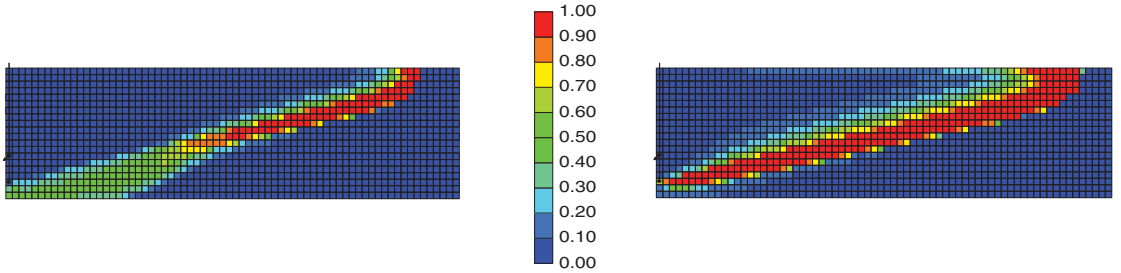

(e) Distributions of the C_5 mole fraction in the *L* phase for C_5-steam coinjection at 2 years; Left: C_5 concentration of 1 mol%, Right: C_5 concentration of 8 mol%. Continuous coinjection of a high-concentration solvent results in an unfavorably thick region of solvent accumulation. This can lead to a significant amount of solvent being trapped near the chamber edge by the end of process.

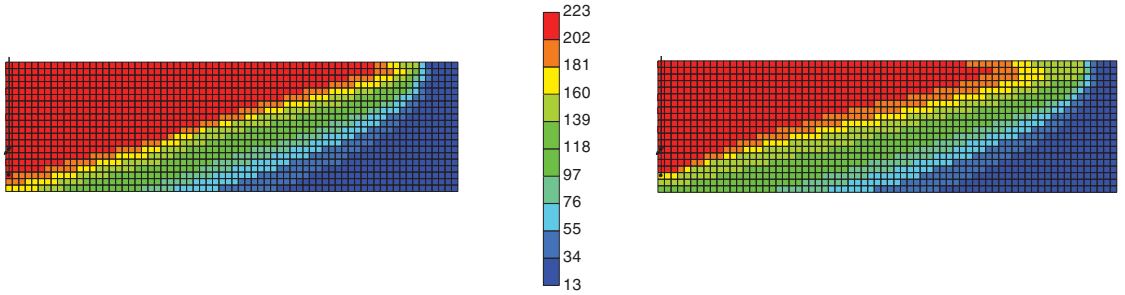

(f) Distributions of temperature at 2 year; Left: C_5 concentration of 1 mol%, Right: C_5 concentration of 8 mol%.

Fig. 14 (continued)—Distributions of the *L*-phase saturation, solvent (C_5) mole fraction in the *L* phase, and temperature in solvent/steam-coinjection simulations at 1 and 2 years.

volume of solvent retention can be as much as 20% of the cumulative bitumen production for continuous coinjection of a fixed solvent concentration.

Retention of solvent inside the reservoir mainly occurs in three places: Place 1, which is the *V* phase inside the chamber; Place 2, which is the *L* phase inside the chamber and at the chamber edge; and Place 3, which is the *L* phase in the unswept region. Solvent retention in Place 2 can be efficiently minimized by maximizing oil recovery. Solvent retention in Place 1 can be significant, depending on reservoir conditions and the solvent coinjected, as is shown in the simulation case for Senlac SAP pilot in the next section. The molar density of the *V* phase is smaller than that of the *L* phase. However, the *L*-phase saturation can be much lower than S_{or} in the regions where displacement efficiency is enhanced as a result of solvent re-evaporation (Keshavarz 2013; Keshavarz et al. 2014). Thus, in the case of volatile-solvent coinjection with steam, solvent retention in the *V* phase can be more significant than that in *L* phase (e.g., more than 90 mol% of the total solvent was observed in the vapor phase at gridblocks in the chamber for the C_3-coinjection case). Solvent retention in Place 3 can occur because of diffusion and dispersion of solvent through the *L* phase, which is difficult to model accurately in the conventional finite-difference simulation. In this section, our focus is on maximizing oil recovery while minimizing the solvent loss in Place 2 by controlling the concentration of solvent in the injectant.

A thicker solvent-rich bank is beneficial for oil recovery, but the main portion of oil drainage occurs within a few meters of the chamber edge, where both heat and solvent-dilution effects contribute (Keshavarz et al. 2014) (Fig. 12). Also, accumulation of solvent in the *V* phase in the chamber lowers the temperature there, as explained in the Condensation Behavior of Steam and Solvent in Coinjection section. That is, solvent accumulation early in the process is beneficial, but a very-thick region of solvent accumulation in the *L* and *V* phases is unfavorable later in the process.

The following coinjection procedure is tested:

- Step 1: Start coinjection of solvent with a high solvent concentration after the thermal communication between the wells is established.
- Step 2: Gradually decrease the solvent concentration in the injectant to avoid a very thick solvent-rich region in situ.
- Step 3: Inject only steam for the final period of the process (e.g., when the chamber reaches the outer boundary for the well pair).

Beginning coinjection with a high solvent concentration in Step 1 expedites accumulation of solvent near the chamber edge early in the process. This contributes to higher oil recovery because of enhanced local-displacement efficiency. A declining trend of the solvent concentration in Step 2 is to control the thickness of the solvent-rich bank near the chamber edge when the chamber is laterally expanding. Termination of solvent coinjection in Step 3 is to prevent the accumulated solvent from being trapped in the *L* phase along the chamber edge.

Fig. 15 compares the injection and production volumes of C_5 in coinjection simulations by use of two different injection procedures. One is to coinject C_5 at a constant concentration of 2 mol% in the injectant throughout the entire process. The other is to vary the solvent concentration in the injectant in a stepwise manner **(Fig. 16).** The variable-concentration case results in 58% less volume of C_5 retention in situ at 5 years.

Fig. 17 shows the volumes of C_5 left in the reservoir and the *L*-phase-saturation distributions after 5 years of operation for the two cases. The variable-concentration case achieves enhanced-displacement efficiency in the chamber and reduces solvent retention at the end of the process. The constant-concentration case yields significant accumulation of C_5 near the outer boundary at the end of the process. Results show that the *L* phase in this region consists of almost 100% C_5. The cumulative oil production at 5 years is 10 147 std m^3 from one-half of the chamber in the constant-concentration case, and 9995 std m^3 for the variable-concentration case. The solvent retention at 5 years is 1293 std m^3 for the constant-concentration case and 533 std m^3 for the variable-concentration case. The variable-concentration case results in improved local-displacement efficiency in the swept region, but its swept region is smaller at 5 years. This is why the variable-concentration case results in 1.3% lower ultimate recovery of bitumen, which is worth a fraction of the improved C_5 recovery.

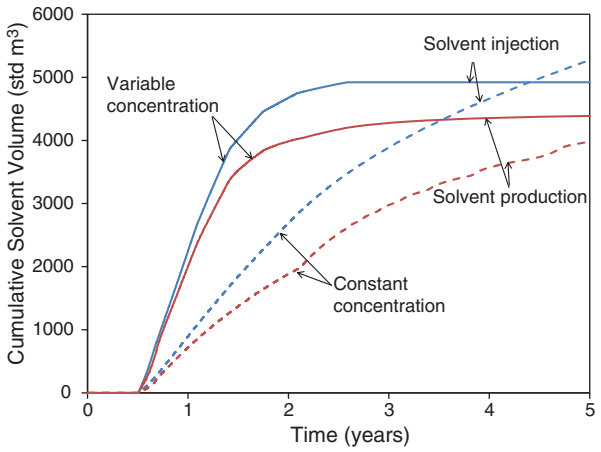

Fig. 15—Injection and production volumes of C_5 in coinjection simulations by use of two different injection procedures. Results correspond to one-half of the chamber. The solid line corresponds to the modified coinjection procedure given in the Design of Solvent Concentration section. The dashed line corresponds to a constant solvent concentration of 2.0 mol%. Solvent recovery is improved from 75.5% in the constant-concentration case to 89.2% in the modified coinjection procedure.

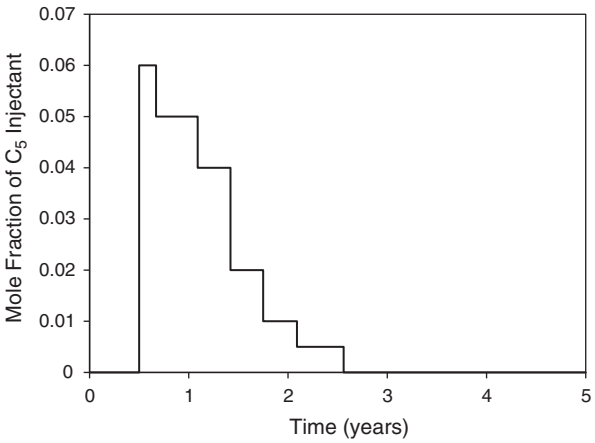

Fig. 16—Variation of the solvent concentration in the injectant during the modified coinjection procedure. C_5 is used as the solvent. Coinjection begins with a high solvent concentration after interwell thermal communication is established. Coinjection is continued with a declining trend of the solvent concentration and is terminated at 2.6 years, when the chamber reaches the lateral boundary for the well pair.

Simulation Case Studies

This section investigates two coinjection pilots: the Senlac solvent-aided-process (SAP) pilot by EnCana and the Long Lake expanding-solvent steam-assisted-gravity-drainage (ES-SAGD) pilot by Nexen. It is indicated in the literature that the results of the former were more encouraging than those of the latter. The main objective here is to clarify the reasons for these mixed results on the basis of the limited information available in the literature. It is also discussed whether any further improvements could have been made for these pilots.

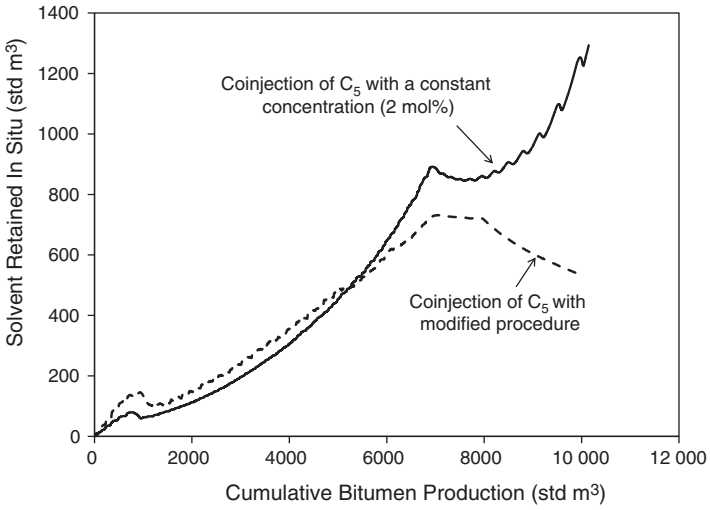

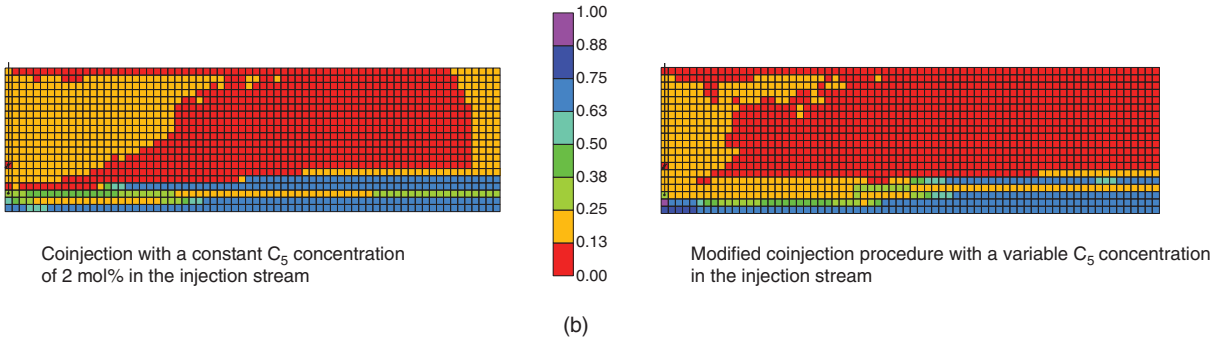

Fig. 17—Volumes of C_5 left in the reservoir and the *L*-phase-saturation distributions after 5 years of operation for the two injection procedures: one with a constant C_5 concentration of 2.0 mol% and the other with a variable C_5 concentration. Results are presented for one-half of the chamber only. Red regions in the *L*-phase-saturation distributions show enhanced local-displacement efficiency. The variable-concentration case can enhance local-displacement efficiency in a wider region.

Properties	Values
Porosity (Boyle et al. 2003)	33%
Horizontal permeability (Boyle et al. 2003)	8,000 md
Vertical permeability (Boyle et al. 2003)	7,000 md
Initial reservoir pressure at depth of 500 (Boyle et al. 2003)	5200 kPa
Initial reservoir temperature (Boyle et al. 2003)	29°C
Initial oil saturation (Boyle et al. 2003)	0.85
Initial water saturation (Boyle et al. 2003)	0.15
Residual oil saturation	0.13
Irreducible water saturation	0.15
Three-phase relative permeability model (CMG 2011)	Stone's Model II
Total pay thickness (Boyle et al. 2003)	16 m
Oil density (Boyle et al. 2003)	985 kg/m^3
Minimum subcool (Gupta et al. 2003)	25°C
Injector bottomhole pressure (maximum)	5250 kPa
Maximum injection rate (includes steam and solvent)	800 t/d
Producer bottomhole pressure (minimum)	5000 kPa
Injection temperature (Gupta et al. 2003)	260°C
Steam quality	0.9

Table 2—Reservoir and fluid data for simulation of Senlac SAP pilot at a depth of 750 m.

Senlac SAP Pilot. EnCana's Senlac SAP pilot was successfully conducted in 2002 at 100 km southeast of Lloydminster, Alberta. The entire project consisted of three phases: Phases A, B, and C. Phase C had two well pairs, C1 and C2, with a horizontal section of 750 m and an interwell-pair spacing of 120 m. A short period of SAP was tested for the Well C1 pair (Boyle et al. 2003). The reservoir oil in this project is not an extraheavy oil, and its viscosity exhibits less sensitivity to temperature than typical bitumen viscosity.

Preheating was performed for approximately 2 months as described in Boyle et al. (2003). After 7 months of SAGD, the SAP pilot began in January 2002 with coinjection of a small amount of C_4 with steam with no significant change in the operational conditions. Gupta et al. (2005) reported a significant increase in the bitumen-production rate from an average of 302 m^3/d (1,900 B/D) during SAGD to an average of 477 m^3/d (3,000 B/D) during the SAP pilot. Also, the steam/oil ratio (SOR) decreased from an average of 2.6 to 1.6 for the same periods.

History matching is conducted for the bitumen-production rate and the SOR for the periods of SAGD and SAP by use of the STARS simulator (CMG 2011). Reservoir/fluid properties and recurrent data are taken from Boyle et al. (2003) and Gupta et al. (2003), as listed in **Table 2.** The dimensions of the reservoir model are 120, 750, and 16 m in the *x*-, *y*-, and *z*-direction, respectively. A uniform gridblock size of $2\times750\times1$ m is used. The reservoir oil is assumed to be a dead oil. Phase-equilibrium calculations are conducted on the basis of *K*-values tabulated before the simulation. The *K*-values are generated by use of the Peng and Robinson (1976) equation of state for hydrocarbon components and by use of Raoult's law for the water component.

Temperature (°C)	Viscosity (cp)
0	104,330
60	396.85
120	23.28
180	4.77
240	1.84
300	1.00

Table 3—Viscosity/temperature behavior for simulation of Senlac SAP pilot.

Adjustments are made on the oil-viscosity/temperature relation, permeabilities in the horizontal and vertical directions, and the solvent concentration in the injectant for SAP. The oil viscosity was reported to be 5,000 cp at reservoir conditions (Boyle et al. 2003). The model of Pedersen and Fredenslund (1987), as implemented in the WinProp software (CMG 2011), was used to match this viscosity and to predict the viscosity/temperature behavior of the oil. **Table 3** shows the adjusted oil viscosity. The permeability of the reservoir was reported to be 5–10 darcies (Boyle et al. 2003). The best matching results were obtained when the horizontal and vertical permeabilities were set to 8 and 7 darcies, respectively.

A fixed concentration of 15% (on the mass basis) of C_4 is selected to match data for the SAP period. Simulation results after history matching are presented in **Fig. 18,** along with data taken from the literature. Reasonable agreements can be observed for the oil-production rate and the SOR between data and simulations. Simulations also exhibited that coinjection of C_4 and steam can significantly increase the production rate from an average of 1,900 to 3,000 B/D, as reported by Gupta et al. (2005). Because of the scarcity of the field data available, no further adjustment of parameters is conducted for the discussion here.

Then, other solvents are tested on the basis of the previously discussed simulation model. The solvent C_4 for the SAP period is replaced with C_3, C_5, or C_6. The molar concentration of solvent is fixed at 5.2%, which is equivalent to 15% of C_4 on the mass basis in the original SAP case. It is assumed that all coinjections, including the C_4 case, are continued for approximately 3 years after the beginning of the SAP pilot on 24 January 2002. **Fig. 19** presents the average oil-production rates for different solvents after 12 months of coinjection (i.e., the SAGD period is not included in calculation of the average production rate). The original solvent selection of C_4 corresponds to the breakover point in Fig. 19, resulting in the highest average oil-production rate. The optimum volatility of coinjection solvent is shifted to the more-volatile side, compared with the case of Athabasca bitumen. This is likely because of the lower sensitivity of the Senlac reservoir-oil viscosity to temperature than that of the Athabasca bitumen at the operating conditions considered in this study.

Now two scenarios are compared: Scenario 1 is the original operation in the Senlac SAP pilot, and Scenario 2 uses the modified injection procedure presented in the previous section. The two scenarios use C_4 as the coinjected solvent. In Scenario 1, solvent coinjection is started after the peak-production rate is

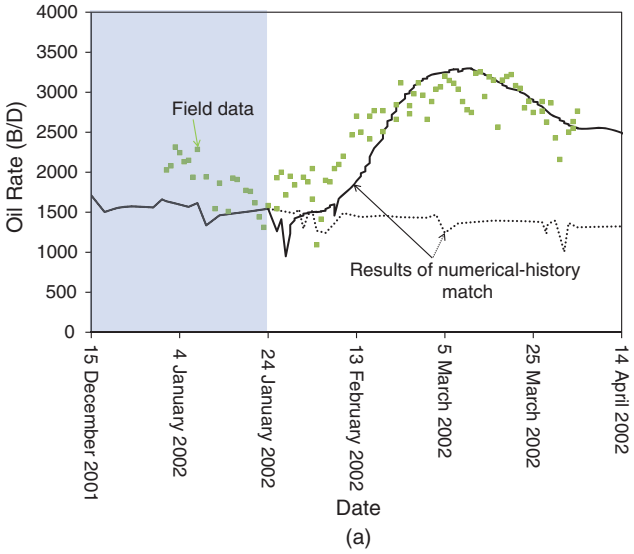

Fig. 18—Field data and results of simulation history matching for Well Pair C1 in the Senlac SAP project in 2002: (a) the bitumen-production rate and (b) the instantaneous SOR. Scattered points are field data reported by Gupta et al. (2005). The period before the SAP test is shaded. The dotted line shows the expected trend of the SAGD performance without SAP. The oil-production rate is reported in B/D for simplicity of comparison with results reported by Gupta et al. The average SOR values for the SAGD period from the pilot and simulation data are 2.6 and 3.2, respectively. These values reduce to 1.6 and 1.8 during the coinjection period, respectively.

achieved in SAGD, and is stopped shortly after the oil-production rate starts decreasing (Gupta and Gittins 2006). Thus, coinjection starts at 24 January 2002 with a C_4 concentration of 5.2 mol%, and continues until 1 April 2002. After that, steam is the only injectant until January 2006. In Scenario 2, coinjection starts with a C_4 concentration of 5.2 mol% immediately after thermal communication is achieved between the wells. The C_4 concentration is then gradually decreased until it becomes zero after 1 year of coinjection.

Fig. 20 compares the two scenarios in terms of the oil-production history and the *L*-phase-saturation distribution at the end of the process. Scenario 2 results in approximately 5.4% additional oil recovery than Scenario 1 by the end of the simulations. Scenario 2 exhibits enhanced oil displacement (i.e., $S_o < S_{or}$) in a wider portion of the reservoir. This is because of earlier accumulation of the solvent near the chamber edge, which is a key requirement for enhanced oil displacement (Keshavarz et al. 2014). These results indicate that it is beneficial to achieve solvent

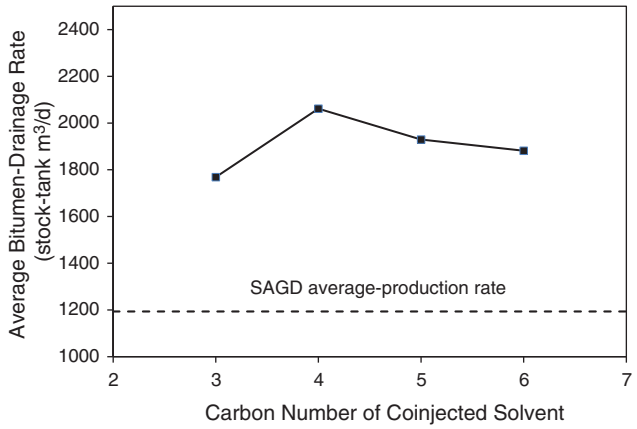

Fig. 19—The average oil-production rates after 12 months of SAP in simulations with different single-component solvents. The SAGD period is not considered in calculation of the average rates. The average oil-production rate for steam-only injection is shown with a horizontal line. The breakover point occurs at C_4, where there is an optimum balance between the heat-transfer effect and the solvent-diluting effect on the oil-drainage rate.

accumulation near the chamber edge as early in the process as possible.

Fig. 21 presents the solvent-injection and -production amounts in Scenario 2. Although the variable-solvent concentration in Scenario 2 attempts to minimize the amount of solvent retention in the *L* phase, solvent recovery is not as successful as the case studied in the previous section. Solvent recovery is only approximately 55.8% because solvent retention in the *V* phase is quite significant in this case.

Comparison of Scenario 2 with the steam-only injection process shown in Fig. 18 indicates that the cumulative oil production can be improved from 265 300 std m^3 to 298 800 std m^3 for 5 years of operation. Scenario 2 also can reduce the cumulative SOR by the end of the fifth year from 4.64 to 3.87. Scenario 2 shows that the C_4 retention is 6856 t at the end of simulation.

Long Lake ES-SAGD Pilot. Long Lake in Athabasca oil sands is approximately 40 km southeast of Fort McMurray. Nexen conducted an SAGD pilot at the Long Lake project site from May 2003 until August 2006. An ES-SAGD test was performed for Well Pair 3 from February 13 to 16 April 2006. This ES-SAGD coinjected Jet B, a mixture of petroleum fractions from C_7 to C_{12}, at a volumetric concentration of 5% except for an initial short period (Orr et al. 2010). The ES-SAGD pilot did not show significant changes in oil-production rate compared with SAGD (Nexen 2007).

A uniform gridblock size of $2\times650\times1$ m^3 is used to model a reservoir with dimensions of $100\times23\times650$ m^3 in the *x*-, *y*-, and *z*-direction, respectively. **Table 4** shows rock and fluid data taken from Nexen's annual report for the Long Lake project (Nexen 2007, 2012; and Orr 2009). *K*-values are generated by use of an equation of state (Peng and Robinson 1976) for hydrocarbon components and by use of Raoult's law for water. Because details of Jet B are unavailable in literature, it is assumed that Jet B behaves similarly to C_{10}, for simplicity. By use of this assumption, 5 vol% of Jet B is equivalent to 0.5 mol% of C_{10} for the coinjection simulation in this subsection. Bitumen viscosities at different temperatures were taken from Orr (2009), as given in **Table 5.**

The injection and production pressures are adjusted to match the SAGD-production data from May 2003 to February 2006. The injection pressure is initially 2800 kPa and follows a declining trend, as reported by Nexen (2007). They are stabilized at approximately 1400 kPa for the ES-SAGD period and afterward. **Fig. 22** shows history-matching results for the SAGD-production rate.

On the basis of the history-matched reservoir/fluid models, the ES-SAGD pilot is simulated with a C_{10} concentration of 0.5

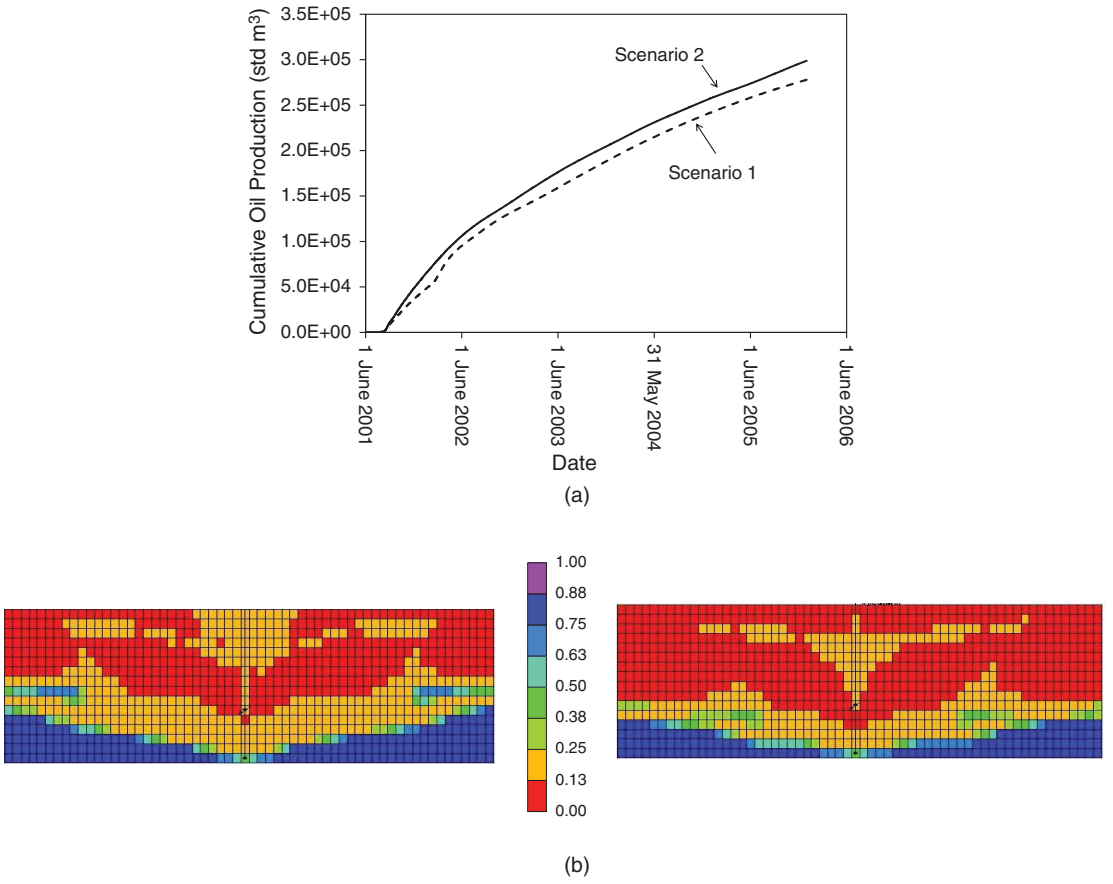

Fig. 20—Comparison of EnCana's original operation (Scenario 1) and a modified coinjection process (Scenario 2) for the Senlac SAP pilot. (a) Cumulative-oil-production histories. (b) Distributions of the *L*-phase saturation at the end of two SAP cases: Scenario 1 is given on the left, and Scenario 2 is given on the right. C_4 is used as an optimum solvent. Regions in red exhibit enhanced displacement efficiency; $S_o < S_{or}$. The modified coinjection procedure results in 5.4% additional oil recovery and improves local-displacement efficiency in a wider portion of the swept region.

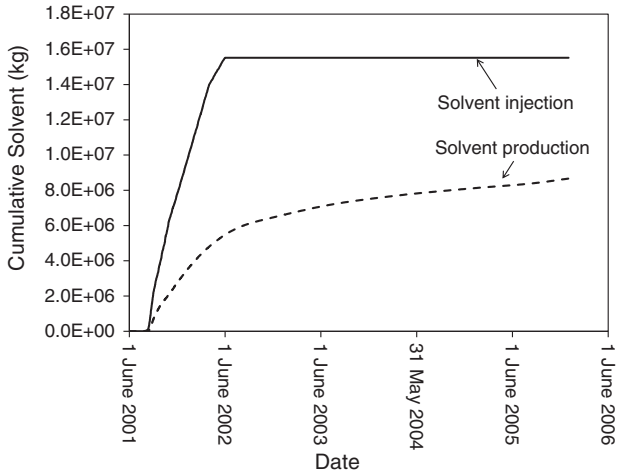

Fig. 21—Cumulative solvent injection and production during SAP with Scenario 2. Coinjection starts with a C_4 concentration of 5.2 mol% immediately after thermal communication is achieved between the wells. Solvent concentration decreases gradually until it becomes zero after 1 year of coinjection. The C_4 amounts are reported on the mass basis because C_4 is produced in the *L* and *V* phases. Although Scenario 2 attempts to lower solvent retention in the *L* phase by the end of the process, the overall solvent recovery is not as successful as the case studied earlier. This is because the main retention of solvent in this case occurs in the *V* phase because of the high volatility of C_4. The ultimate amount of the retained solvent is 6856 t after 5 years.

mol% in the injectant between 13 February 2006 and 16 April 2006. There is no significant change observed in the oil-production rate during the period of coinjection and during the first few months after the termination of coinjection. However, an improvement of 17% in oil-production rate, compared with SAGD, is observed approximately 5 months after the termination of solvent coinjection (Fig. 22). A sufficient accumulation of solvent near the chamber edge is one of the keys to successful coinjection, as explained by Keshavarz et al. (2014), which was not achieved within 2 months in this ES-SAGD simulation.

The procedure presented in this paper for selecting a single-component solvent is implemented. Here, it is assumed that coinjection began on 13 February 2006 and continued for 4 years. The same reservoir model is used with different single-component solvents at a concentration of 2.0 mol%. **Fig. 23** shows that the average bitumen-production rate for 1 year of coinjection exhibits a breakover point at C_5. Therefore, Jet B used in Nexen's ES-SAGD pilot is likely a suboptimum solvent because of its low volatility. Ardali et al. (2012b) speculated that the low volatility of Jet B is the reason for the less-encouraging results of the Long Lake ES-SAGD pilot. Fig. 23, however, shows that C_{10}, a single-component solvent equivalent to Jet B, can exhibit a higher oil-production rate than SAGD once a sufficient amount is injected.

Comparisons are made between two scenarios. Scenario 1 attempts to follow the actual operation by Nexen. Coinjection of C_{10} is conducted with a constant concentration of 0.5 mol% after the initial SAGD period between May 2003 and February 2006. This coinjection is continued for 2 months. After that, only steam is injected until January 2010. In Scenario 2, coinjection of C_5 is started after the interwell communication is achieved in July 2003. The solvent concentration is initially 5.0 mol%, and then is

Properties	Values
Porosity	31%
Horizontal permeability	6,300 md
Vertical permeability	4,900 md
Initial reservoir pressure at depth of 200	1050 kPa
Initial reservoir temperature	7°C
Initial oil saturation	0.68
Initial water saturation	0.32
Residual oil saturation	0.13
Irreducible water saturation	0.25
Three-phase relative permeability model	Stone's Model II
Total pay thickness	23 m
Oil density	930 kg/m^3
Minimum subcool	10°C
Steam quality	0.9

Table 4—Reservoir and fluid data for simulation of Long Lake ES-SAGD pilot at a depth of 200 m.

Temperature (°C)	Viscosity (cp)
0	7,708,500
75	2691
150	68.19
225	9.94
300	3.30

Table 5—Viscosity/temperature behavior for simulation of Long Lake ES-SAGD pilot.

reduced in a stepwise manner. Coinjection is stopped after approximately 2 years, when the chamber reaches the boundaries of the reservoir model.

Fig. 24 compares the two scenarios in terms of oil production and local-displacement efficiency. Scenario 2 yields 22% higher oil recovery than Scenario 1 at January 2010. The steam chamber in Scenario 2 propagates faster than that in Scenario 1 by exploiting the effects of solvent accumulation near the chamber edge from the early stage of the process. This is the main reason for the significant improvement observed in the cumulative oil production in Fig. 24. Another reason is that Scenario 2 gives higher local-displacement efficiency in the chamber (regions in red in Fig. 24b) than Scenario 1 because of sufficient solvent accumulation near the chamber edge. **Fig. 25** presents the cumulative amounts of solvent injected and produced in Scenario 2. Results show that 83.4% of the coinjected-solvent volume can be recovered by the end of the process.

Comparison of Scenario 2 with the steam-only injection process shown in Fig. 22 indicates an improvement of the cumulative oil production from 156 300 std m^3 to 220 300 std m^3 after 6.7 years of operation. The cumulative SOR is also reduced from 6.05 to 4.14 by this time. Scenario 2 results in the C_5 retention of 5365 t at the end of the simulation.

Economic Analysis

In previous sections, some key guidelines for designing the coinjection processes were provided to maximize the average production rate, enhance the displacement efficiency, and minimize the solvent retention (dynamic and ultimate) in the *L* phase. This section provides a limited economic analysis to investigate whether the technical success of the proposed guidelines can lead to an economic success.

The simulation cases previously presented for steam-assisted gravity drainage (SAGD), C_3/steam, C_5/steam, and C_8/steam coinjections are considered in this section. However, the well length is

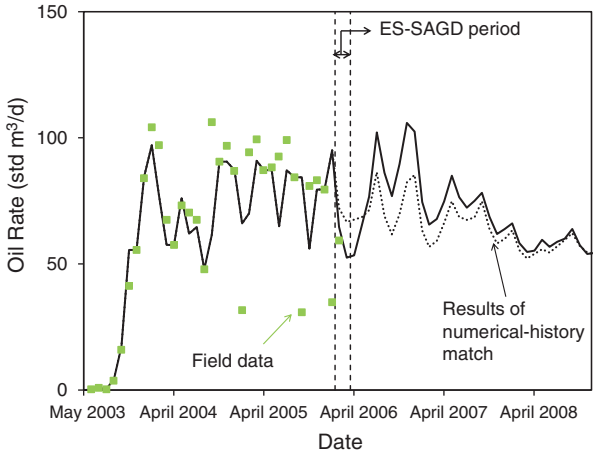

Fig. 22—Field data and results of history matching for oil-production rate from Well Pair 3 for the Long Lake SAGD/ES-SAGD project. Scattered points are field data reported by Orr (2009). The bold curve shows simulated bitumen-production rate. ES-SAGD is conducted in February and March 2006. C_{10} is continuously coinjected with steam, with a C_{10} concentration of 0.5 mol% for this period. The dashed curve shows the forecasted trend of oil production in SAGD with no ES-SAGD.

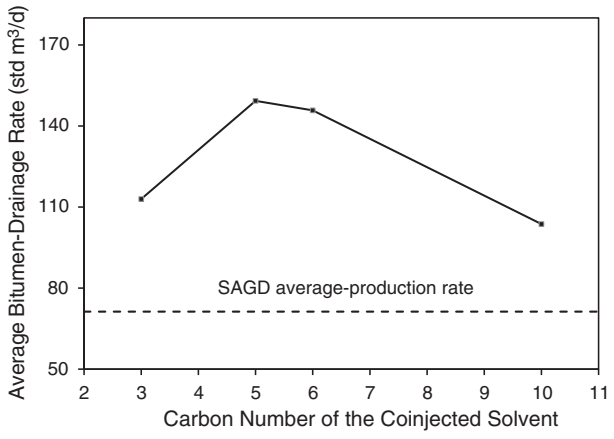

Fig. 23—Average oil-production rates for 1 year of the Long Lake ES-SAGD with different single-component solvents. The SAGD period is not considered in calculation of the average rates. The average oil-production rate for steam-only injection (i.e., SAGD) is shown as a horizontal line. The breakover point is observed at C_5, where there is an optimum balance between the heat-transfer effect and the solvent-diluting effect on the oil-drainage rate.

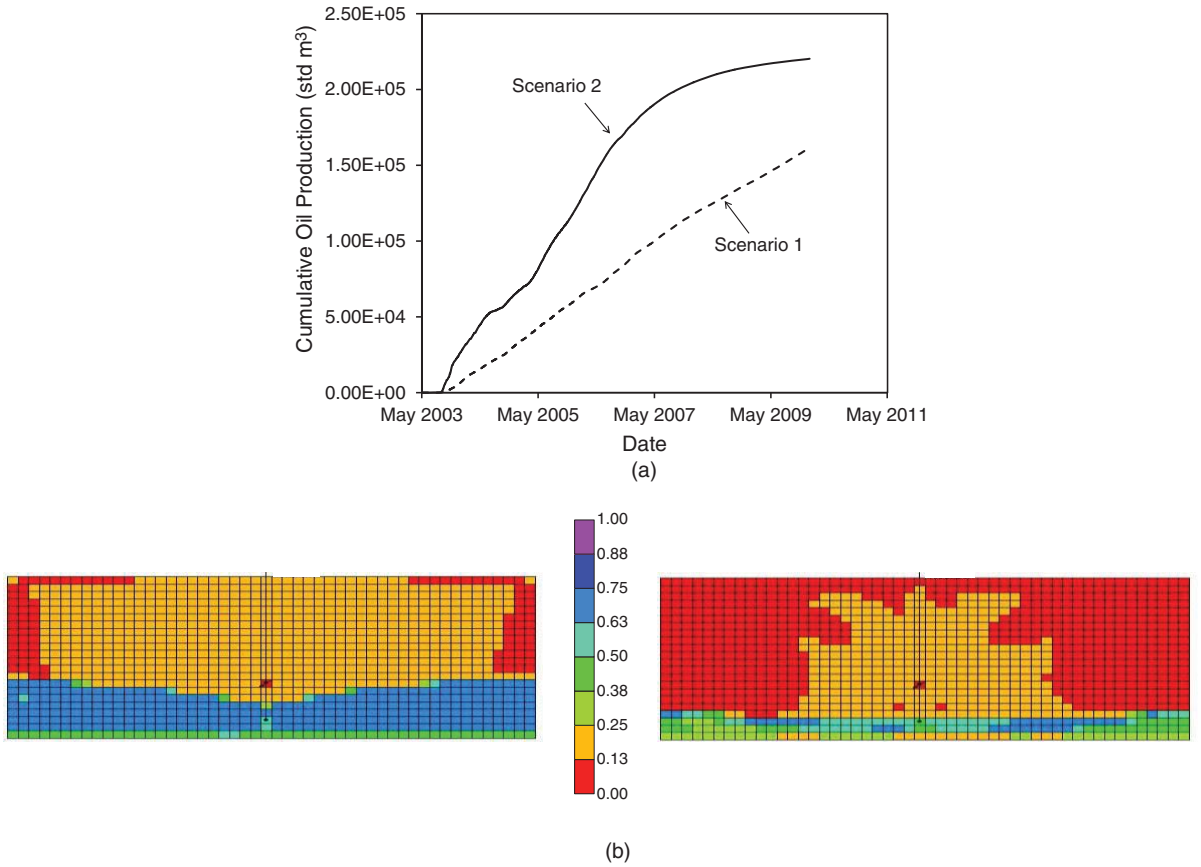

Fig. 24—Comparison between Nexen's original process (Scenario 1) and the modified coinjection (Scenario 2) for the Long Lake ES-SAGD pilot. (a) Cumulative-bitumen-production histories. (b) Distributions of the *L*-phase saturation at 6.6 years. Scenario 1 is given on the left and Scenario 2 on the right. Solvent production as part of the *L* phase is excluded in calculations of cumulative production. Results indicate that Scenario 2 yields 22% more oil recovery than Scenario 1 by January 2010. Scenario 2 exhibits faster chamber propagation and a wider region of local-displacement-efficiency improvement. Regions in red in (b) exhibit enhanced displacement efficiency, where the *L*-phase saturation is lower than the input residual oil saturation.

increased from 37.5 to 500 m. This is to better represent the economic performance at the well-pair scale. Solvent is coinjected with a constant concentration of 2.0 mol% in the injectant unless otherwise stated.

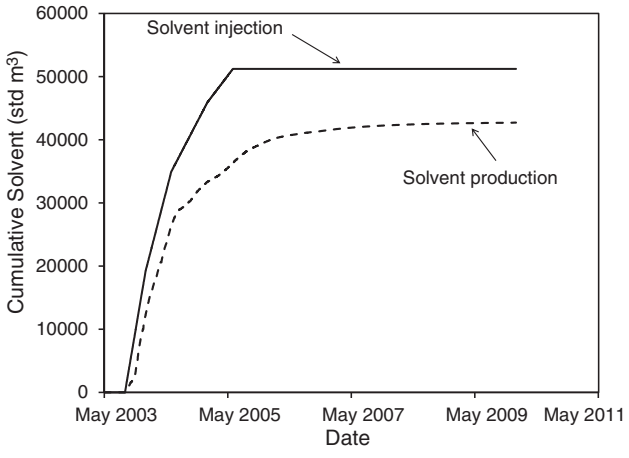

Fig. 25—Injection and production volumes of solvent for Scenario 2 for the Long Lake ES-SAGD simulation. Coinjection starts with 5.0 mol% of solvent in the injectant. Solvent concentration is then decreased in a stepwise manner. Part of the accumulated solvent in the chamber is recovered after the termination of solvent coinjection in June 2005. Results indicate that more than 80% of the injected solvent is recovered. The ultimate solvent retained in situ is 5365 t by January 2010.

A simple cumulative supply-cost model is defined as follows:

$$
\begin{aligned}
&\text{Net present value (NPV) (USD)}\\
&= (\text{cumulative oil} \times \text{oil price})\\
&\quad \times (1.0 - \text{discount rate})(\text{USD})\\
&\quad - \text{capital cost of exploration (USD)}\\
&\quad - \text{capital cost of well pair (USD)}\\
&\quad - \text{water} - \text{treament equipment (USD)}\\
&\quad - \text{steam} - \text{generator cost (USD)}\\
&\quad - \text{capital cost of solvent distribution (USD)}\\
&\quad - \text{administration and head office (USD)}\\
&\quad - \text{blending and transportation (USD)}\\
&\quad - \text{production years (years)}\\
&\quad \times \text{well pair and field operation (USD/yr)}\\
&\quad - \text{production years (years)} \times \text{solvent handling (USD/yr)}\\
&\quad - \text{cumulative steam injection}\\
&\qquad [\text{m}^3 \text{ cold water equivalent (CWE)}]\\
&\quad \times [\text{generator operation (USD/m}^3 \text{ CWE)}\\
&\quad + \text{fuel cost (USD/m}^3 \text{ CWE)}]\\
&\quad - \text{cumulative water production (m}^3)\\
&\quad \times \text{treatment of production water} \left(\frac{\text{USD}}{\text{m}^3}\right)\\
&\quad - [\text{cumulative solvent injection (kg)}\\
&\quad - \text{cumulative solvent production (kg)}]\\
&\quad \times \text{solvent price (USD/kg)}.
\end{aligned}
$$

The model takes into account the capital investment and operating costs of a typical SAGD process and additional solvent-related costs with a fixed discount rate over a period of time. It is

Exploration	USD200,00
Well-pair completion	USD4,800/m
Steam generator	USD2,260,000
Water-treatment equipment	USD1,000,000
Solvent-distribution line	USD100,000
Discount rate	0.12
Well-pair and field operation	USD150,000/yr
Administration and head office	USD7.48/m^3 oil
Blending and transportation	USD6.29/m^3 oil
Steam-generator operation	USD2.83/m^3 (CWE)
Fuel for steam generator	USD10.1/m^3 (CWE)
Treatment of water production	USD1.96/m^3
Solvent handling	USD20,00/yr
C_3 price	USD317/liquid m^3
C_5 price	USD397/liquid m^3
C_8 price	USD443/liquid m^3
Oil price	USD80/bbl

Key: CWE = cold-water equivalent.

Table 6—Input parameters used in economic analysis.

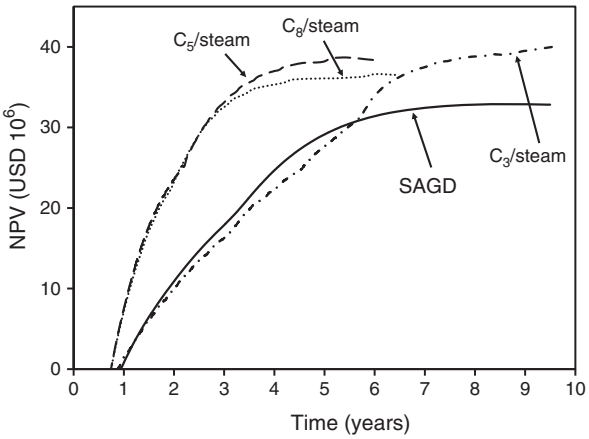

Fig. 26—Comparison of NPV for SAGD and three coinjection cases. Solvents are coinjected at a constant concentration of 2.0 mol% throughout the project time.

assumed that there is no reservoir-gas production because of the very-heavy nature of the bitumen used in the simulations. The values used for this economic analysis are partly taken from Deng (2005) and presented in **Table 6.** The cost for fuel to generate steam is modeled after the heat price of USD3.35/million Btu (Deng 2005).

Fig. 26 compares the NPV for SAGD and three different coinjection cases. Each curve shows the NPV until some time after the maximum value is achieved. **Table 7** compares the duration and the water demand of SAGD and the three coinjection processes at the same bitumen-recovery factor. The rightmost two columns compare the costs of steam (including fuel, steam-generator operating, and water treatment) and the retained solvent for the cases. A considerable portion of the operation costs belong to steam generation and water treatment. The coinjection cases show reductions in the steam demand compared with SAGD. Thus, they are likely to be more promising than SAGD. The superior economic performance can be seen for the C_5 and C_8 coinjection cases in Fig. 26. As discussed in previous sections, the C_3-coinjection case exhibits slower chamber growth than the C_5/steam-coinjection and C_8/steam-coinjection cases, as can be also seen in Fig. 26. Coinjection of C_5 with steam results in a slightly better economic performance than that of C_8. This is mainly because of the lower cumulative steam/oil ratio.

Table 7 shows that the final costs associated with the solvent loss can be comparable with those of steam generation and water treatment if coinjection is continued at a constant solvent concentration in the injectant throughout the project. However, the process is still much faster with C_5 or C_8 coinjection than with SAGD. Fig. 26 shows that the time required for the C_3-steam coinjection to achieve a comparable NPV is almost twice that for the other coinjection cases studied. **Table 8** presents the maximum NPV for each process as well as the corresponding project time at which this maximum is achieved. According to this table, C_5 is likely the best solvent choice for these simple simulation cases.

Fig. 27 compares the NPV for SAGD and two C_5/steam-coinjection cases: one with a constant solvent concentration (2.0 mol%) and the other with a modified coinjection strategy to improve the displacement efficiency and solvent recovery, as described in previous sections. A blowdown phase is considered at the final stage of SAGD and the C_5/steam coinjection with the modified coinjection strategy. Production is continued for a few months without any injection during the blowdown. This has improved the maximum NPV of SAGD by USD0.90 million compared with the case presented in Table 8. For the coinjection case, an additional 680 m^3 of C_5 is recovered as part of the produced oil during this blowdown phase.

The benefits of using the modified coinjection strategy are partially offset by the higher steam demand in the third year because of the reduced solvent concentration in the injectant. The maximum NPV is USD70.63 million for SAGD, USD80.52 million for the C_5 coinjection with a constant C_5 concentration, and USD85.55 million for the C_5 coinjection with the modified coinjection strategy. The latter coinjection design results in improvements of 21.1 and 6.2% in the maximum NPV, compared with the SAGD and the former coinjection case, respectively.

Conclusions

A systematic procedure was presented for selecting an optimum solvent and its concentration in coinjection of a single-component solvent with steam. The optimization considered the oil-production rate, ultimate oil recovery, and solvent retention in situ. Conclusions are as follows:

- Reduction of the chamber-edge temperature in coinjection can be qualitatively explained by use of a simplified representation of water/solvent binary phase behavior. The temperature reduction can occur as a direct consequence of deviation of the three-phase temperature from the steam temperature at the injection pressure in water/solvent binary phase behavior.
- Numerical simulation was conducted to quantitatively examine the accuracy of the simplified estimation of the chamber-edge temperature. Results show that the mutual solubility between

Process	Recovery Factor	Time (years)	Cumulative Water Injected (m^3 CWE)	Retained-Solvent Cost (USD)	Steam Cost (USD)
SAGD	0.65	4.97	1 192 887	0	17,750,562
C_3/steam coinjection	0.65	4.93	549 680	12,742,052	8,159,910
C_5/steam coinjection	0.65	2.46	611 811	9,622,152	9,073,416
C_8/steam coinjection	0.65	2.49	731 211	7,429,396	10,862,928

Table 7—Economic comparison of SAGD and three solvent/steam coinjections in terms of steam and solvent costs.

Process	Maximum NPV (USD 10^6)	Duration (years)
SAGD	69.73	8.81
C_3/steam coinjection	83.76	9.58
C_5/steam coinjection	80.52	5.44
C_8/steam coinjection	76.72	6.07

Table 8—Economic comparison of SAGD and three steam/solvent coinjections.

the dead oil and solvent and fluids' nonidealities can substantially affect physical properties at the chamber edge.

- The chamber-edge-temperature reduction becomes more significant for coinjection of a more-volatile solvent with steam for given operating conditions. A less-volatile solvent, however, results in a more-viscous mixture when mixed with bitumen at a given mixing ratio at a temperature and pressure. Thus, an optimum volatility of solvent can be typically observed in terms of the oil-production rate for given operating conditions. Different reservoir/fluid properties result in different optimum solvents.
- A key to enhanced oil recovery in coinjection is accumulation of solvent in the oleic phase outside the chamber. It is possible to maximize oil recovery and minimize solvent retention in situ by controlling the concentration of a given coinjection solvent. Beginning coinjection immediately after achieving interwell communication enables the enhancement of oil recovery early in the process. Subsequently, the solvent concentration should be gradually decreased until it becomes zero for the final period of the coinjection. This coinjection procedure can minimize solvent retention in the oleic phase in situ (both dynamic and ultimate) while keeping oil recovery.
- The proposed guidelines were successfully applied to simulation of the Senlac solvent-aided-process pilot project, which is one of the successful field applications of solvent/steam coinjection. Results indicate that the original solvent selection of C_4 is the optimum solvent in terms of the oil-production rate for this project. Although local-displacement efficiency and solvent recovery can be further improved by modifying the coinjection procedure, the incremental-oil recovery is insignificant.
- The proposed guidelines were also applied to simulation of the Long Lake expanding-solvent steam-assisted-gravity-drainage (ES-SAGD) project. The main reason for this less successful ES-SAGD is likely that 2 months of coinjection at a low solvent concentration gave an insufficient amount of solvent accumulation near the chamber edge. Also, Jet B seems to be a suboptimum solvent for this ES-SAGD. The proposed guidelines indicate that C_5 is the optimum solvent in terms of oil-production rate. Simulation results for coinjection of C_5 with a variable solvent concentration show that oil recovery can be enhanced by 22% compared with the original operation scheme and that 83.4% of injected solvent can be recovered by the end of the process.
- A limited economic analysis showed that steam/solvent coinjection has a potential to improve the economics of bitumen recovery compared with SAGD when the proposed guidelines are used for solvent selection and concentration design.

Nomenclature

L = oleic phase
N_C = number of components
P = pressure, kPa or bar
P_{inj} = injection pressure, kPa or bar
P^{vap} = vapor pressure, kPa or bar
S_o = oil saturation
S_{or} = residual oil saturation
T = absolute temperature, K
T_{inj} = injection temperature
T_{3p} = oleic/gaseous/aqueous equilibrium
V = gaseous phase
W = aqueous phase

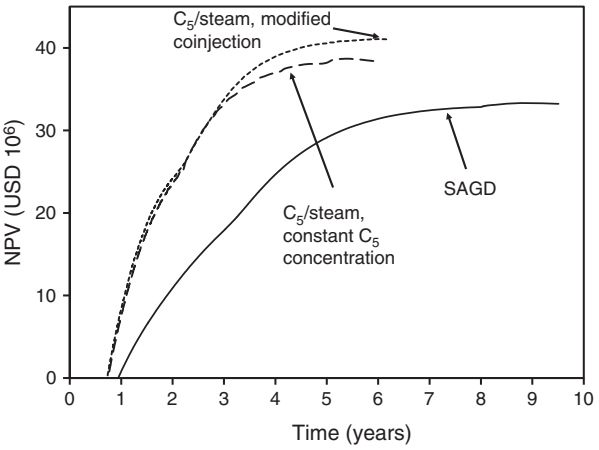

Fig. 27—Comparison of NPV for SAGD and two C_5/steam-coinjection scenarios: one with a constant concentration of C_5 (2.0 mol%) in the injectant and the other with the modified coinjection strategy. A blowdown phase is considered in the final stage of the SAGD and C_5/steam coinjection with the modified coinjection strategy.

x = molar concentration
y = mole fraction in the vapor phase
μ = viscosity, cp

Subscripts

i = component index
j = phase index
solvent = solvent component
water = water component

Acknowledgments

A partial support for this research was obtained from author Babadagli's Natural Sciences and Engineering Research Council Industrial Research Chair in Unconventional Oil Recovery (industrial partners are Schlumberger, Canadian Natural Resources Ltd., Suncor Energy, Petrobank, Sherritt Oil, Apex Engineering, and Pemex). Ryosuke Okuno gratefully acknowledges a partial financial support from the Natural Sciences and Engineering Research Council for this research (RGPIN No. 418266).

References

Adepoju, O.O., Lake, L.W., and Johns, R.T. 2013. Investigation of Anisotropic Mixing in Miscible Displacements. *SPE Res Eval & Eng* **16** (1): 85–96. SPE-159557-PA. http://dx.doi.org/10.2118/159557-PA.

Ardali, M., Barrufet, M., and Mamora, D.D. 2012a. Laboratory Testing of Addition of Solvents to Steam to Improve SAGD Process. Presented at SPE Heavy Oil Conference Canada, Calgary, Alberta, Canada, 12–14 June. SPE-146993-MS. http://dx.doi.org/10.2118/146993-MS.

Ardali, M., Barrufet, M.A., Mamora, D.D., et al. 2012b. A Critical Review of Hybrid Steam/Solvent Processes for the Recovery of Heavy Oil and Bitumen. Presented at SPE Annual Technical Conference and Exhibition, San Antonio, Texas, 8–10 October. SPE-159257-MS. http://dx.doi.org/10.2118/159257-MS.

Ardali, M., Mamora, D.D., and Barrufet, M. 2010. A Comparative Simulation Study of Addition of Solvents to Steam in SAGD Process. Presented at Canadian Unconventional Resources and International Petroleum Conference, Calgary, Alberta, Canada, 19–21 October. SPE-138170-MS. http://dx.doi.org/10.2118/138170-MS.

Boyle, T.B., Gittins, S.D., and Chakrabarty, C. 2003. The Evolution of SAGD Technology at East Senlac. *J Can Pet Technol* **42** (1): 58–61. PETSOC-03-01-06. http://dx.doi.org/10.2118/03-01-06.

Butler, R.M. 1997. *Thermal Recovery of Oil and Bitumen*. Calgary, Alberta, Canada: GravDrain Inc.

Canbolat, S. and Akin, S. 2002. A Study of Steam-Assisted Gravity Drainage Process in the Presence of Noncondensable Gases. Presented at

SPE/DOE Improved Oil Recovery Symposium, Tulsa, Oklahoma, 13–17 April. SPE-75130-MS. http://dx.doi.org/10.2118/75130-MS.

CMG. 2011. *STARS Version 2011 User Guide*. Calgary, Alberta, Canada: CMG.

Deng, X. 2005. Recovery Performance and Economics of Steam/Propane Hybrid Process. Presented at the SPE International Thermal Operations and Heavy Oil Symposium, Calgary, Alberta, Canada, 1–3 November. SPE-97760-MS. http://dx.doi.org/10.2118/97760-MS.

Dong, L. 2012. Effect of Vapor-Liquid Phase Behavior of Steam-Light Hydrocarbon Systems on Steam Assisted Gravity Drainage Process for Bitumen Recovery. *Fuel* **95** (May): 159–168. http://dx.doi.org/10.1016/j.fuel.2011.10.044.

Edmunds, N., Moini, B., and Peterson, J. 2010. Advanced Solvent-Additive Processes by Genetic Optimization. *J Can Pet Technol* **49** (9): 34–41. SPE-140659-PA. http://dx.doi.org/10.2118/140659-PA.

Garmeh, G. and Johns, R.T. 2010. Upscaling of Miscible Floods in Heterogeneous Reservoirs Considering Reservoir Mixing. *SPE Res Eval & Eng* **13** (5): 747–763. SPE-124000-PA. http://dx.doi.org/10.2118/124000-PA.

Gates, I.D. 2007. Oil Phase Viscosity Behavior in Expanding-Solvent Steam-Assisted Gravity Drainage. *J. Petrol. Sci. Eng.* **59** (1–2): 123–134. http://dx.doi.org/10.1016/j.petrol.2007.03.006.

Gates, I.D. and Chakrabarty, N. 2008. Design of Steam and Solvent Injection Strategy in Expanding Solvent Steam-Assisted Gravity Drainage. *J Can Pet Technol* **47** (9): 12–19. PETSOC-08-09-12-CS. http://dx.doi.org/10.2118/08-09-12-CS.

Gates, I.D. and Gutek, A.M.H. 2008. *Process for In Situ Recovery of Bitumen and Heavy Oil*. US Patent No. 7,464,756.

Govind, P.A., Das, S.K., Srinivasan, S., et al. 2008. Expanding Solvent SAGD in Heavy Oil Reservoirs. Presented at SPE International Thermal Operations and Heavy Oil Symposium, Calgary, Alberta, Canada, 20–23 October. SPE-117571-MS. http://dx.doi.org/10.2118/117571-MS.

Gupta, S., and Gittins, S.D. 2012. An Investigation Into Optimal Solvent Use and the Nature of Vapor/Liquid Interface in Solvent-Aided SAGD Process With a Semianalytical Approach. *SPE J.* **17** (4): 1255–1264. SPE-146671-PA. http://dx.doi.org/10.2118/146671-PA.

Gupta, S. and Gittins, S.D. 2006. Christina Lake Solvent Aided Process Pilot. *J Can Pet Technol* **45** (9): 15–18. PETSOC-06-09-TN. http://dx.doi.org/10.2118/06-09-TN.

Gupta, S.C. and Gittins, S.D. 2007b. Effect of Solvent Sequencing and Other Enhancements on Solvent Aided Process. *J Can Pet Technol* **46** (9): 57–61. PETSOC-07-09-06. http://dx.doi.org/10.2118/07-09-06.

Gupta, S. and Gittins, S. 2007a. Optimization of Solvent Aided Process. Presented at the Canadian International Petroleum Conference, Calgary, Alberta, Canada, 12–14 June. PETSOC-2007-022. http://dx.doi.org/10.2118/2007-022.

Gupta, S., Gittins, S. and Picherack, P. 2005. Field Implementation of Solvent Aided Process. *J Can Pet Technol* **44** (**11**): 8–13. PETSOC-05-11-TN1. http://dx.doi.org/10.2118/05-11-TN1.

Gupta, S., Gittins, S. and Picherack, P. 2003. Insights into Some Key Issues with Solvent Aided Process. *J Can Pet Technol* **43** (2): 54–61. PETSOC-04-02-05. http://dx.doi.org/10.2118/04-02-05.

Hosseininejad Mohebati, M., Maini, B.B., and Harding, T.G. 2010. Optimization of Hydrocarbon Additives with Steam in SAGD for Three Major Canadian Oil Sand Deposits. Presented at the Canadian Unconventional Resources and International Petroleum Conference, Calgary, Alberta, Canada, 19–21 October. SPE-138151-MS. http://dx.doi.org/10.2118/138151-MS.

Ivory, J., Zheng, R., Nasr, T., et al. 2008. Investigation of Low Pressure ES-SAGD. Presented at SPE International Thermal Operations and Heavy Oil Symposium, Calgary, Alberta, Canada, 20–23 October. SPE-117759-MS. http://dx.doi.org/10.2118/117759-MS.

Jha, R.K., Kumar, M., Benson, I., et al. 2013. New Insights into Steam/Solvent-Coinjection-Process Mechanism. *SPE J.* **18** (5): 867–877. SPE-159277-PA. http://dx.doi.org/10.2118/159277-PA.

Jiang, H., Deng, X., Huang, H., et al. 2012. Study of Solvent Injection Strategy in ES-SAGD Process. Presented at SPE Heavy Oil Conference Canada, Calgary, Alberta, Canada, 12–14 June. SPE-157838-MS. http://dx.doi.org/10.2118/157838-MS.

Jiang, Q., Butler, R., and Yee, C.T. 1998. The Steam and Gas Push (SAGP)-2: Mechanism Analysis and Physical Model Testing. Presented at Annual Technical Meeting, Calgary, Alberta, Canada, 8–10 June. PETSOC-98-43. http://dx.doi.org/10.2118/98-43.

Keshavarz, M. 2013. *Mechanistic Simulation Study of Steam-Solvent Coinjection for Bitumen and Heavy-Oil Recovery*. MS thesis, University of Alberta, Edmonton, Alberta, Canada (July 2013).

Keshavarz, M., Okuno, R., and Babadagli, T. 2014. Efficient Oil Displacement Near the Chamber Edge in ES-SAGD. *J. Petrol. Sci. Eng.* **118** (June): 99–113. http://dx.doi.org/10.1016/j.petrol.2014.04.007.

Leaute, R.P. 2002. Liquid Addition to Steam for Enhancing Recovery of Bitumen with CSS: Evolution of Technology from Research Concept to a Field Pilot at Cold Lake. Presented at SPE International Thermal Operations and Heavy Oil Symposium and International Horizontal Well Technology Conference, Calgary, Alberta, Canada, 4–7 November. SPE-79011-MS. http://dx.doi.org/10.2118/79011-MS.

Leaute, R.P. and Carey, B.S. 2005. Liquid Addition to Steam for Enhancing Recovery (LASER) of Bitumen with CSS: Results from the First Pilot Cycle. Presented at Canadian International Petroleum Conference, Calgary, Alberta, Canada, 7–9 June. PETSOC-2005-161. http://dx.doi.org/10.2118/2005-161.

Li, W. and Mamora, D.D. 2010. Phase Behavior of Steam with Solvent Co-injection under Steam Assisted Gravity Drainage (SAGD) Process. Presented at the SPE EUROPEC/EAGE Annual Conference and Exhibition, Barcelona, Spain, 14–17 June. SPE-130807-MS. http://dx.doi.org/10.2118/130807-MS.

Li, W., Mamora, D.D., and Li, Y. 2011a. Light-and Heavy-Solvent Impacts on Solvent-Aided-SAGD Process: A Low-Pressure Experimental Study. *J Can Pet Technol* **50** (4): 19–30. SPE-133277-PA. http://dx.doi.org/10.2118/133277-PA.

Li, W., Mamora, D.D., and Li, Y. 2011b. Solvent-Type and -Ratio Impacts on Solvent-Aided SAGD Process. *SPE Res Eval & Eng* **14** (3): 320–331. SPE-130802-PA. http://dx.doi.org/10.2118/130802-PA.

Linstorm, P.J., and Mallard, W.G. 2011. *National Institute of Standards and Technology (NIST) Chemistry WebBook*, NIST Standard Reference Database No. 69, http://webbook.nist.gov (accessed 1 October 2012).

Mehrotra, A.K. and Svrcek, W.Y. 1986. Viscosity of Compressed Athabasca Bitumen. *Can. J. Chem. Eng.* **64** (5): 844–847. http://dx.doi.org/10.1002/cjce.5450640520.

Mehrotra, A.K. and Svrcek, W.Y. 1987. Corresponding States Method for Calculating Bitumen Viscosity. *J Can Pet Technol* **26** (5): 60–66. PETSOC-87-05-06. http://dx.doi.org/10.2118/87-05-06.

Mohammadzadeh, O., Rezaei, N., and Chatzis, I. 2012. More Insight into the Pore-Level Physics of the Solvent-Aided SAGD (SA-SAGD) Process for Heavy Oil and Bitumen Recovery. Presented at SPE Heavy Oil Conference Canada, Calgary, Alberta, Canada, 12–14 June. SPE-157776-MS. http://dx.doi.org/10.2118/157776-MS.

Nasr, T.N. and Ayodele, O.R. 2006. New Hybrid Steam-Solvent Processes for the Recovery of Heavy Oil and Bitumen. Presented at Abu Dhabi International Petroleum Exhibition and Conference, Abu Dhabi, UAE, 5–8 November. SPE-101717-MS. http://dx.doi.org/10.2118/101717-MS.

Nasr, T.N., Beaulieu, G., Golbeck, H., et al. 2003. Novel Expanding Solvent-SAGD Process "ES-SAGD." *J Can Pet Technol*, **42** (1): 13–16. PETSOC-03-01-TN. http://dx.doi.org/10.2118/03-01-TN.

Nexen Inc., 2007. Annual Performance Presentation for Long Lake Oil Sand Scheme & Long Lake annual Resource Management Report, http://www.aer.ca/documents/oilsands/insitu-presentations/2007AthabascaNexenLongLakeSAGD_9151_9485.pdf (accessed 18 April 2013).

Nexen Inc., 2012. Long Lake 2011-Subsurface Performance Presentation. ERCB's database. http://www.aer.ca/documents/oilsands/insitu-presentations/2012AthabascaNexenLongLakeSAGD9485.pdf (accessed 18 April 2013).

Orr, B. 2009. ES-SAGD; Past, Present and Future. Presented at the SPE Annual Technical Conference and Exhibition, New Orleans, Louisiana, 4–7 October. SPE-129518-STU. http://dx.doi.org/10.2118/129518-STU.

Orr, B.W., Srivastava, P., Sadetsky, V., et al. 2010. Reducing Steam Oil Ratio in Steam-Assisted Gravity Drainage. Presented at the Canadian Unconventional Resources and International Petroleum Conference,

Calgary, Alberta, Canada, 19–21 October. SPE-136851-MS. http://dx.doi.org/10.2118/136851-MS.

Pedersen, K.S. and Fredenslund, A. 1987. An Improved Corresponding States Model for the Prediction of Oil and Gas Viscosities and Thermal Conductivities. *Chem. Eng. Sci.* **42** (1): 182–186. http://dx.doi.org/10.1016/0009-2509(87)80225-7.

Peng, D.-Y. and Robinson, D.B. 1976. A New Two-Constant Equation of State. *Ind. Eng. Chem. Fundamen.* **15** (1): 59–64. http://dx.doi.org/10.1021/i160057a011.

Rachford, H.H. Jr. and Rice, J.D. 1952. Procedure for Use of Electronic Digital Computers in Calculating Flash Vaporization Hydrocarbon Equilibrium. *J Pet Technol* **4** (10): 19–3. SPE-952327-G. http://dx.doi.org/10.2118/952327-G.

Redford, D.A. and McKay, A.S. 1980. Hydrocarbon-Steam Processes for Recovery of Bitumen from Oil Sands. Presented at SPE/DOE Enhanced Oil Recovery Symposium, Tulsa, Oklahoma, 20–23 April. SPE-8823-MS. http://dx.doi.org/10.2118/8823-MS.

Shu, W.R. and Hartman, K.J. 1988. Effect of Solvent on Steam Recovery of Heavy Oil. *SPE Res Eng* **3** (2): 457–465. SPE-14223-PA. http://dx.doi.org/10.2118/14223-PA.

Yazdani, A., Alvestad, J., Kjonsvik, D., et al. 2011. A Parametric Simulation Study for Solvent Co-injection Process in Bitumen Deposits. Presented at the Canadian Unconventional Resources Conference, Calgary, Alberta, Canada, 15–17 November. SPE-148804-MS. http://dx.doi.org/10.2118/148804-MS.

Appendix A—Example Calculation for Three-Phase Temperature

An example calculation is presented for T_{3p} and y_i by use of Eqs. 1 and 2. C_4 is used as the solvent component in this example. The vapor-pressure curves of water and C_4 are given by the following correlations:

$$P^{\text{vap}}_{\text{H}_2\text{O}} = 100 \times 10^{\left(3.55959 - \frac{643.748}{T - 198.043}\right)}, \quad (379\ \text{K} < T < 573\ \text{K}), \qquad \text{(A-1)}$$

$$P^{\text{vap}}_{\text{C}_4} = 100 \times 10^{\left(4.35576 - \frac{1175.581}{T - 2.071}\right)}, \quad (273\ \text{K} < T < 425\ \text{K}), \qquad \text{(A-2)}$$

where P is pressure in kPa and T is temperature in Kelvin. At an operating pressure of 3000 kPa, Eq. 2 can be written as

$$3{,}000 = 100 \times \left(10^{3.55959 - \frac{643.748}{T - 198.043}} + 10^{4.35576 - \frac{1175.581}{T - 2.071}}\right), \qquad \text{(A-3)}$$

which results in T_{3p} of 131°C. The vapor pressure of water and butane are calculated to be 277 kPa and 2723 kPa at this temperature, respectively. The corresponding mole fraction of each component in the V phase can be approximated by use of Eq. 2 as

$$y_{\text{H}_2\text{O}} = \frac{P^{\text{vap}}_{\text{H}_2\text{O}}}{P} = 0.09$$

and $y_{\text{C}_4} = \frac{P^{\text{vap}}_{\text{C}_4}}{P} = 0.91.$

Conversion Factors

atm × 1.013 250*	E+05 = Pa
bar × 1.0*	E+05 = Pa
bbl × 1.589 873	E−01 = m^3
cp × 1.0*	E−03 = Pa·s
ft × 3.048*	E−01 = m
°F (°F−32)/1.8	= °C
°F (°F + 459.67)/1.8	= K
psi × 6.894 757	E+00 = kPa

*Conversion factor is exact.

Mohsen Keshavarz is a PhD degree candidate in the Department of Chemical and Petroleum Engineering at the University of Calgary. His main area of research is analytical and numerical modeling of thermal and solvent/thermal recovery processes. Keshavarz is a member of SPE and the Canadian Society of Petroleum Geologists. He holds a bachelor's degree in petroleum engineering from Sharif University of Technology, Iran, and a master's degree in petroleum engineering from the University of Alberta.

Ryosuke Okuno has served as an assistant professor of petroleum engineering in the Department of Civil and Environmental Engineering at the University of Alberta since 2010. His research and teaching interests include enhanced oil recovery, thermal oil recovery, oil-displacement theory, numerical reservoir simulation, thermodynamics, multiphase behavior, and applied mathematics. Okuno has 7 years of industrial experience as a reservoir engineer with Japan Petroleum Exploration Company and is a registered professional engineer in Alberta, Canada. He is a recipient of the 2012 SPE Petroleum Engineering Junior Faculty Research Initiation Award. Okuno holds bachelor's and master's degrees in geosystem engineering from the University of Tokyo and a PhD degree in petroleum engineering from the University of Texas at Austin.

Tayfun Babadagli is a professor in the Department of Civil and Environmental Engineering at the University of Alberta, where he holds the Natural Sciences and Engineering Research Council Industrial Research Chair in Unconventional Oil Recovery. Babadagli previously served on the faculty at Istanbul Technical University, Turkey, and Sultan Qaboos University, Oman. His areas of interest include modeling fluid and heat flow in heterogeneous and fractured reservoirs, reservoir characterization through stochastic and fractal methods, optimization of oil/heavy-oil recovery by conventional/unconventional enhanced-oil-recovery methods, and carbon dioxide sequestration. Babadagli was an executive editor for *SPE Reservoir Evaluation and Engineering* (Formation Evaluation part) between 2010 and 2013 and currently is an associate editor of *ASME Journal of Energy Resources Technology*. He was an SPE Distinguished Lecturer in 2013–14 and was elected as an SPE Distinguished Member in 2013. Babadagti has served on the technical program and steering committees of 13 SPE conferences and forum series and on the SPE Education and Professionalism and SPE Career Guidance and Student Development committees. He holds bachelor's and master's degrees from Istanbul Technical University and master's and PhD degrees from the University of Southern California, all in petroleum engineering.